Afferent-specific modulation of excitatory synaptic transmission by acetylcholine and serotonin in the prelimbic cortex

Arielle L. Baker and Allan T. Gulledge*

Affiliations:

1. Department of Molecular and Systems Biology
   Geisel School of Medicine at Dartmouth College
   Hanover, NH 03755

Running title: Neuromodulation of excitatory afferents in the prelimbic cortex

Keywords: Prefrontal cortex, Acetylcholine, Serotonin, Pyramidal neuron, Mediodorsal nucleus, Synaptic transmission, Neuromodulation, EPSP

* *To whom correspondence should be addressed*
Department of Molecular and Systems Biology
Geisel School of Medicine at Dartmouth College
74 College Street, Vail 601
Hanover, NH 03755
Phone: (603) 646-5249
email: allan@dartmouth.edu

Abstract

Acetylcholine (ACh) and serotonin (5-hydroxytryptamine, or 5-HT) differentially regulate the excitability of pyramidal neurons in the mouse prelimbic (PL) cortex according to their long-distance projections. We tested for afferent- and/or target-specific modulation of glutamate release by these neuromodulators in two key afferents to the PL cortex: commissural (COM) projections from the contralateral hemisphere and projections from the mediodorsal nucleus (MDN) of the thalamus. Using an ex-vivo optogenetic approach, we mapped the connectivity of COM and MDN afferents in intratelencephalic (IT) and extratelencephalic (ET) layer 5 projection neurons and tested for afferent-selective neuromodulation of synaptic transmission. Dual whole-cell recordings in pairs of IT and ET neurons found that COM afferents monosynaptically target both IT and ET neurons, but that MDN afferents selectively target IT neurons. Both afferents exhibited similar, and target-independent, short-term synaptic plasticity (facilitation), but were differentially modulated by ACh and 5-HT. COM transmission was suppressed strongly by ACh and moderately by 5-HT, while MDN inputs to IT neurons were largely unaffected by either neuromodulator. Cholinergic suppression of COM transmission was blocked by atropine or the M4-preferring antagonist VU602841, but enhanced by the M4 positive allosteric modulator VU0467154. Serotonergic suppression of COM transmission was mildly reduced in the presence of SB216691, a 5-HT_{1B} receptor antagonist. Chemogenetic inhibition of hM4Di-expressing COM terminals mimicked the suppressive effects of ACh and 5-HT on synaptic transmission. These data demonstrate that, while ACh and 5-HT differentially regulate IT and ET excitability, they are similarly selective in regulating COM synaptic transmission in the PL cortex.

Introduction

Acetylcholine (ACh) and serotonin (5-hydroxytryptamine, or 5-HT) are chemical transmitters in the neocortex that promote cognition primarily by modulating, rather than driving, neural circuits (for reviews, see Puig and Gulledge, 2011; Colangelo et al., 2019). In the mouse prelimbic (PL) cortex, ACh and 5-HT reciprocally modulate the excitability of two subtypes of layer 5 pyramidal neurons: intratelencephalic (IT) neurons that project bilaterally within the cerebrum, and extratelencephalic (ET; also known as "pyramidal tract", or PT) neurons that extend unilateral corticofugal projections to the midbrain and brainstem (Tudi et al., 2024). Whereas ACh preferentially enhances the excitability of ET neurons via G_q-coupled M1-type muscarinic ACh receptors (Gulledge et al., 2009; Dembrow et al., 2010; Baker et al., 2018; Gulledge, 2024), 5-HT acts at 5-HT_{1A} (1A; $G_{i/o}$-coupled) receptors to inhibit ET neurons while simultaneously increasing the excitability IT neurons via 5-HT_{2A} (2A; G_q-coupled) receptors (Avesar and Gulledge, 2012; Stephens et al., 2014; Elliott et al., 2018; Stephens et al., 2018). Thus, cortical release of ACh is expected to enhance ET-dependent corticofugal output, while 5-HT release may preferentially promote intracortical and corticostriatal circuits while simultaneously inhibiting corticofugal output.

G_q-coupled metabotropic receptors, such as M1 and 2A receptors, typically have little direct impact on quiescent pyramidal neurons, but increase the gain of responses to excitatory synaptic drive (Andrade, 1991; Araneda and Andrade, 1991; Baker et al., 2018; Stephens et al., 2018; Williams and Fletcher, 2019). Because glutamatergic synapses in the neocortex can express presynaptic receptors, including receptors for ACh and 5-HT, that modulate excitatory synaptic transmission (e.g., Murakoshi et al.,

2001; for reviews, see Schicker et al., 2008; Betke et al., 2012; Yang et al., 2021), predicting the net effect of a neuromodulator on cortical circuit function requires a detailed understanding of both pre- and postsynaptic mechanisms, and their interactions, across a range of cortical neuron subtypes and local and long-distance afferents.

To date, little is known about afferent-specific neuromodulation of glutamate release in the PL cortex, especially with regard to projection-specific target neuron subtypes. In the PL cortex, 5-HT (3 - 30 μM) was found to suppress glutamatergic transmission at COM terminals targeting pyramidal neurons (Kjaerby et al., 2016), but not those innervating fast-spiking interneurons (Athilingam et al., 2017), suggesting the potential for target-specific neuromodulation of COM afferents. In the mouse anterior cingulate cortex, excitatory postsynaptic currents (EPSCs) evoked by electrical stimulation of putative COM afferents were modestly suppressed by 10 or 40 μm 5-HT (Troca-Marin and Geijo-Barrientos, 2010; see also Tian et al., 2017). Consistent with serotonergic suppression of intracortical excitatory connections, 5-HT modestly suppressed unitary synaptic transmission between pyramidal neurons in the prefrontal (layer 5; Rama, 2023) and somatosensory (layer 2; Agahari and Stricker, 2021, 2025) cortexes of young (< 3-weeks old) rats. Serotonergic modulation of thalamocortical transmission has been less studied, but two studies reported serotonergic suppression of thalamocortical transmission in the somatosensory cortex of very young mice that is reduced (Rhoades et al., 1994) or eliminated (Laurent et al., 2002) in adolescence.

Presynaptic cholinergic receptors also regulate glutamate release in the neocortex. In the PL cortex, ACh has been reported to bidirectionally modulate synaptic

transmission in superficial pyramidal neurons, with activation of nicotinic-type ACh receptors enhancing, but muscarinic receptors suppressing, electrically evoked (Vidal and Changeux, 1993) and unitary (Yang et al., 2020) excitatory postsynaptic potentials (EPSPs). Bidirectional cholinergic modulation of excitatory transmission was found to be afferent-specific in the somatosensory cortex, with electrically evoked putative corticocortical synapses being suppressed by mAChR activation, but putative thalamocortical inputs modulated by both mAChRs and nicotinic receptors (Gil et al., 1997; see also Hsieh et al., 2000).

These data suggest a rich substrate for potential afferent- and/or target-specific presynaptic modulation of excitatory synaptic transmission in the PL cortex that may work in concert to promote or suppress information flow in defined cortical circuits. Here we employ an optogenetic approach to compare target neuron selectivity and presynaptic modulation of glutamate release by ACh and 5-HT in COM and MDN afferents to the PL cortex. Our results demonstrate that excitatory afferents to the PL cortex can selectively target specific projection neuron subtypes and that afferent-, but not target-specific, modulation of glutamate release may interact with projection-specific postsynaptic signaling to preferentially engage specific cortical-striatal-thalamic circuits.

Methods

Animals and ethical approvals

Experiments utilized female and male 7- to 24-week-old C57BL/6J mice according to protocols approved by the Institutional Animal Care and Use Committee of Dartmouth College. Mice were bred and cared for in dedicated facilities accredited by the Association for

Assessment and Accreditation of Laboratory Animal Care. With food and water continuously available, mice experienced a 12-hour light-dark cycle and were housed with littermates until surgery (see below). Post surgery, animals were housed individually until use in experiments.

Animal surgeries

Intracranial injections were used to deliver adeno-associated viruses (AAVs) encoding channelrhodopsin-2 (ChR2) or chemogenetic tools to specific neuron populations. During surgeries, mice were anesthetized with vaporized isoflurane (~2%), given an intraperatoneal (IP) injection of ketoprofen as an analgesic (4 mg/kg), and secured in a stereotaxic frame. Craniotomies were made according to age-appropriate coordinates (**Table 1**), and a microsyringe lowered into the brain region of interest (medial prefrontal cortex [mPFC] or mediodorsal nucleus [MDN] of the thalamus), and infusions of AAV viruses made at a rate of 50 nL per minute. Mice were allowed to recover from surgery for at least 3 weeks prior to use in electrophysiology experiments. Accuracy of injection sites was confirmed via visualization of m-cherry in coronal brain sections of the PL cortex or thalamus.

Slice preparation

Anesthetized mice (2% vaporized isoflurane) were decapitated and their brains removed rapidly into carbogen- (95% O_2 / 5% CO_2) saturated artificial cerebral spinal fluid (aCSF) composed of (in mM): 125 NaCl, 25 $NaHCO_3$, 3 KCl, 1.25 $NaH2PO_4$, 0.5 $CaCl_2$, 6 $MgCl_2$, and 25 glucose. Coronal slices (250 µm thick) were cut with a vibratome (Leica VT 1200) and stored in holding chambers filled with aCSF containing 2 mM $CaCl_2$ and 1 mM $MgCl_2$. Slices were left to recover for ~45 minutes at 35°C, and then stored at room temperature (~26°C) until use in experiments.

Electrophysiology

Slices were transferred to a low-volume (~1 ml) recording chamber perfused continuously (~5 ml / min) with warm (35 - 36°C) carbogen-saturated aCSF under an Olympus upright

microscope. Using a 60x objective and oblique illumination, layer 5 cortical neurons in the PL cortex were visually targeted for whole-cell current-clamp recording. Patch pipettes (5-7 MΩ) were filled with a solution containing (in mM): 135 potassium gluconate, 2 NaCl, 2 $MgCl_2$, 10 HEPES, 3 Na_2ATP, and 0.3 NaGTP, pH 7.2 with KOH. Recordings were achieved with either BVC-700 amplifiers (Dagan Corporation) and Axograph software (AxoGraph Company) or dPatch amplifiers running SutterPatch software in Igor Pro (Sutter Instrument). Electrode capacitance and series resistance were maximally compensated and membrane potential sampled at 25 kHz (filtered at 5 or 10 kHz) and corrected for the liquid junction potential of +12 mV. Use of current-clamp allowed the physiological classification of IT and ET neurons, action potential generation, and avoided the significant distortion of synaptic events that occurs when voltage-clamp is attempted in pyramidal neurons (e.g., Williams and Mitchell, 2008; Dembrow et al., 2015; Beaulieu-Laroche and Harnett, 2018).

To control for variable levels of ChR2 expression across mice, and to determine relative strength of excitatory afferents to specific postsynaptic neuron subtypes, simultaneous dual recordings were made of IT and ET neurons (typically within 75 µm of each other) in most experiments. IT and ET neurons were identified as previously described according to their physiological characteristics (Gulledge, 2024)(see also Elliott et al., 2018). Briefly, neurons were classified based on a “Physiology Index” (PI) determined from physiological properties that are influenced by the differential expression of hyperpolarization-activated and cyclic nucleotide-gated (HCN) channels in IT and ET neurons (e.g., Sheets et al., 2011; Avesar and Gulledge, 2012; Oswald et al., 2013). The PI was computed for each neuron according to the following formula:

$$PI = \frac{sag(\%) \times slope\text{-}of\text{-}sag(\frac{mV}{s})}{R_N(M\Omega)}$$

where R_N is the neuron’s input resistance, “sag” is the relative magnitude of the steady state HCN-mediated rebound in membrane potential to a 20 mV (peak) hyperpolarizing current

injection (as a percent of the peak hyperpolarization), and “slope-of-sag” is the rate of voltage rebound as determined by linear regression over a 50 ms period beginning at the time of peak hyperpolarization (see **Table 2**). Neurons with a PI of greater than 4.5 were identified as ET, while those with a PI lower than 3.5 were identified as IT. Neurons with intermediate PIs were excluded from analysis (Gulledge, 2024).

EPSPs were optically evoked using LED-driven epifluorescent flashes of blue (460 or 470 nm; 1 ms) light with the 60x objective over layer 5. LED intensities were measured at the objective with a LaserCheck intensity meter (model 45-018; Edmond Optics). EPSPs were typically evoked in pairs at 20 Hz to measure short-term plasticity, with flashes repeated at 15 s intervals to allow for recovery from short-term plasticity. Measurements of EPSP characteristics were made from averaged responses of ten consecutive trials in each experimental condition. EPSP amplitudes were measured relative to the mean resting membrane potential in the 50 ms prior to the initial light flash, while measurements of EPSP onset latency (determined at 5% amplitude) were made relative to the onset of light flashes. EPSP width (which is primarily a measure of decay kinetics) was made at half peak amplitude relative to baseline membrane potential.

In most experiments, LED power was adjusted such that the first of the two EPSPs was ~10 mV in amplitude while still allowing for a subthreshold second EPSP. For comparisons of afferent targeting, only IT-ET pairs in which at least one neuron had an EPSP ≥ 5 mV were used for analyses. Resting membrane potentials were maintained throughout experiments using slow DC current injection (manually, or using the dynamic holding function of the dPatch). Pharmacological agents (e.g., ACh, 5-HT) were bath applied for 7 minutes with measurements made from the average of the final 10 EPSPs in each experimental condition. Pharmacological manipulations were followed by a 15-20 minute wash period. For dose-response experiments, normalized mean data were fit with a Hill equation using Igor Pro’s CurveFit function and constraining to an assumed null effect at 1 pM concentration. For data with ACh, where all concentrations except for “eserine-only” generated suppression greater than 50%, we first fit the

raw data with an initial Hill equation (that “converged properly”), and then used that curve to estimate the eserine-only concentration of ACh (139 nM), before fitting a final Hill equation to the mean data including the eserine-only estimate.

Pharmacological agents

Most substances were dissolved in water to make stock solutions (typically at 10,000x concentration) that were frozen as aliquots and used as needed during experiments. Acetylcholine (Fisher Scientific) was bath-applied with 10 μM physostigmine hemisulfate (eserine; Tocris Bioscience), a blocker of acetylcholinesterase. 4-aminopyridine (4-AP) was purchased from Fisher, while atropine was obtained from Sigma Aldrich. Tetrodotoxin (TTX) citrate and clozapine N-oxide (CNO) hydrochloride were purchased from HelloBio, Inc., and SB 216641 (a 5-HT_{1B} receptor antagonist) was purchased from Abcam. DMSO-based stock solutions were made of VU 6028418 hydrochloride (an M4 receptor antagonist; Tocris Bioscience), AF-DX 116 (an M2 antagonist; Tocris Bioscience), and VU0467154 (an M4 positive allosteric modulator; MedChemExpress).

Statistical Analysis

Unless otherwise noted, data are presented as mean values ± standard deviation. Two-tailed Student’s t-tests for paired or un-paired data were used, as appropriate, to compare physiological responses across experimental condition or across neuron subtype, but no assumptions were made regarding the “significance” of differences in means (see Nieuwenhuis et al., 2011; e.g., Wasserstein et al., 2019). Instead, we quantified effect size as Cohen’s *d*, a measure of standardized mean difference, according to the following formulas:

for non-paired data:

$$d = \frac{|(\bar{x}_A - \bar{x}_B)|}{\sqrt{\frac{(n_A - 1)SD_A^2 + (n_B - 1)SD_B^2)}{n_A + n_B - 2}}}$$

where $\bar{x}_A$ and $\bar{x}_B$ are the mean values of a given parameter (e.g., EPSP amplitude), SD_A and SD_B are the standard deviations for those parameters, and n_A and n_B are the number of observations (i.e., neurons) in each group, or,

for paired data:

$$d = \frac{|\bar{x}_d|}{S_d}$$

where $\bar{x}_d$ is the mean paired difference of a parameter and S_d is the standard deviation of the paired differences. By convention, effect sizes ≥ .8 are considered "large" (i.e., having distributions that overlap by ~50% or less), whereas values of ~0.5 and ~0.2 are considered to be "medium" or "small" effects, respectively, according to their greater (~67% and ~85%) overlap of distributions (Cohen, 1988).

Results

Targeting of IT and ET neurons by commissural and thalamocortical afferents

Dual whole-cell recordings and ChR2-assisted circuit mapping (Petreanu et al., 2007) was used to quantify the relative targeting of IT and ET neurons by commissural (COM; n = 99 IT-ET pairs) or thalamocortical (MDN; n = 58 IT-ET pairs) afferents to the PL cortex (**Figure 1A**-**D**; **Table 3**). Afferent-specific synaptic transmission was triggered with two brief (1 ms) flashes of blue light with a 50 ms inter-flash interval (20 Hz), repeated every 15 s. Flash-evoked EPSPs were sensitive to LED intensity (**Figure 1C**, **E**) and, with the exception of MDN inputs to ET neurons, had short (< 2 ms) onset latencies (**Table 3**). When LED intensities were adjusted to generate, as closely as possible, ~10 mV initial EPSPs across both neurons, while still allowing for subthreshold EPSPs on the second flash, COM EPSPs were slightly larger than those recorded

simultaneously in ET neurons, while paired-pulse ratios (PPRs) were similar across target neuron subtypes (**Figure 1D**, **E**; **Table 3**). These data suggest that COM afferents robustly form synapses with similar short-term plasticity among layer 5 IT and ET target neurons in the PL cortex.

Selective activation of ChR2-expressing MDN afferents generated target-specific responses in IT-ET neuron pairs (**Figure 1C**, **D**). Flash-evoked MDN EPSPs had faster onset latencies in IT neurons (~2 ms) relative to ET neurons (~3 ms; **Table 3**) that were similar to those observed for COM afferents in both IT ($n = 157$; $p = 0.219$, $d = 0.22$) and ET ($p = 0.257$, $d = 0.20$) target neurons. On the other hand, onset latencies for MDN EPSP in ET neurons were delayed relative to MDN EPSPs in IT neurons (**Table 3**) or for COM EPSP onset latencies measured in either ET ($p < 0.001$, $d = 1.31$) or IT ($p < 0.001$; $d = 1.32$) target neurons. MDN EPSPs measured in ET neurons were also smaller in amplitude and exhibited greater paired-pulse facilitation than MDN EPSPs occurring in IT neurons (**Figure 1D**, **E**; **Table 3**) or COM EPSPs recorded in ET ($p < 0.001$; $d = 0.63$) or IT ($p < 0.001$; $d = 0.70$) neurons.

The longer onset latencies and greater PPR for MDN transmission to ET neurons suggest that MDN-evoked responses in ET neurons may result from polysynaptic excitatory drive within the local network (see also Collins et al., 2018). Indeed, flash-evoked EPSPs were often sufficient to drive action potentials (APs) in postsynaptic neurons, especially at higher LED intensities, or on the second of two flashes (**Figure 1F**, **G**). In 18 IT-ET pairs experiencing flash-evoked COM inputs across a range of LED intensities, APs were rarely observed at lower intensities but became progressively more likely as intensities were increased. At the highest LED intensity, APs were more

likely to occur in ET neurons (**Figure 1G**). On the other hand, activation of MDN inputs was more likely to generate APs in IT neurons at lower light intensities, but was equally potent in driving APs in IT and ET neurons at the highest LED intensity (n = 16 IT-ET pairs; **Figure 1G**).

The results described above suggest that optical activation of either COM or MDN afferents may tigger local network activity that may contribute to flash-evoked EPSPs. To compare monosynaptic targeting of IT and ET neurons by COM and MDN afferents, we used TTX (1 μM) to block network activity and 4-AP (100 μM; Petreanu et al., 2009) and increased LED intensities to allow direct ChR2-evoked release from synaptic terminals (**Figure 2A**; see also below). In the presence of TTX and 4-AP, monosynaptic COM EPSPs were robust in both IT and ET target neurons, being slightly larger in the former (**Figure 2B**), while paired-pulse ratios in both target neuron subtypes were substantially reduced relative to those observed in baseline conditions (**Figure 2C**; **Table 4**). The drop in PPR in the presence of TTX and 4-AP, which was also reported by Cruikshank et al. (2010), likely reflects the slow kinetics of ChR2-mediated depolarization of synaptic terminals.

When we isolated monosynaptic MDN inputs with TTX and 4-AP, light-evoked responses in ET neurons became very small and were sometimes undetectable, while EPSPs remained substantial in IT neurons (**Figure 2A**, **B**; **Table 4**). As was true for COM inputs, the addition of TTX and 4-AP reduced PPRs for MDN EPSPs (**Figure 2C**, **Table 4**). These data confirm that MDN-evoked responses in ET neurons are largely polysynaptic.

To explore the frequency dependence short-term synaptic plasticity, in additional neurons (not necessarily dual recordings) we optically evoking trains of ten COM (IT and ET targets) or MDN (IT targets) EPSPs at 10, 20, or 40 Hz (**Figure 3A**, **B**). For both COM and MDN inputs, and across all frequencies and target neuron subtypes, initial responses exhibited facilitation of similar magnitude peaking during the 2nd (for 10 Hz), 2nd or 3rd (for 20 Hz), or 3rd-5th (for 40 Hz) light flash before becoming smaller toward the end of the trains. These results are comparable to those of Martinetti et al., (2022), who reported that paired-pulse facilitation of long-distance ipsilateral corticocortical connections that peaks at ~20 Hz. Only during the final four EPSPs at 10 Hz was there a small difference between COM and MDN inputs (in IT target neurons), but the effect size was small, ranging from 0.34 to 0.38 across the final four EPSPs (**Figure 3B**). Short-term plasticity for COM afferents was also very similar across target neurons, differing only slightly (maximum effect size of 0.25 for response 9) at the end of 40 Hz trains that generated highly variable responses trial-to-trial. These data confirm that short-term plasticity is frequency dependent in COM and MDN afferents, but that synaptic dynamics are largely target-independent. Finally, we confirmed that flash-evoked COM (**Figure 3C**) and MDN (**Figure 3D**) EPSPs were stable over at least 30 minutes of recording (n = 6 IT and 6 ET neurons for each afferent, not necessarily in pairs). The stability of MDN-triggered, mostly polysynaptic responses in ET neurons over time (see above), suggests stability of network dynamics in our acute slices over at least 30 minutes.

Neuromodulation of COM and MDN afferents

To test whether ACh and 5-HT differentially modulate COM and MDN synaptic transmission according to target neuron subtype, recordings were made from pairs of IT and ET target neurons while EPSPs were optically evoked (2x at 20 Hz at 15 s intervals) in baseline conditions and after exposure to either 20 μM ACh (with 10 μM eserine; **Figure 4A** - **C**) or 40 μM 5-HT (**Figure 4D** - **F**). When COM EPSPs were challenged with ACh (n = 8 IT-ET pairs), optically evoked EPSPs were reversibly reduced to a similar extent in IT and ET target neurons (by ~85 ± 5%; **Table 5**), while PPRs increased similarly in both target neuron subtypes ($p = 0.560$, $d = 0.34$, when comparing the magnitude of changes in PPR across afferents; **Figure 4A**,**B**; **Table 5**). These data suggest that ACh acutely suppresses COM synaptic transmission in a target-independent manner.

ACh had more modest effects on optically evoked MDN EPSPs (n = 13 IT-ET pairs; **Figure 4B**, **C**), with the first of two EPSPs being reduced by only ~25% (**Table 5**) and the second EPSPs being reduced by slightly larger amounts, leaving PPRs relatively unchanged in the presence of ACh (**Figure 4B**, **C**; **Table 5**). When cholinergic effects were compared across afferents, COM EPSPs were more sensitive to ACh than MDN inputs ($p < 0.001$, $d = 2.28$; **Figure 4G**; **Table 5**), and only COM inputs demonstrated increased PPRs in the presence of ACh (**Figure 4H**; **Table 5**). Responses to ACh in both afferents were larger than changes observed over time in our experiments in which EPSPs were measured at similar time points but without ACh (see **Figure 3C**, **D**; mean normalized first EPSP amplitudes 10 minutes after baseline measurements was 1.00 ± 0.19 for 24 neurons; $p < 0.001$, $d = 5.57$ when compared to ACh effects on COM

afferents (n = 16 neurons); $p < 0.001$, $d = 3.64$, for ACh effects on MDN afferents measured in 13 IT target neurons; **Figure 4G**, **H**). These data suggest that ACh preferentially suppresses glutamate release at COM terminals but does not have target-specific effects.

We next tested the impact of 5-HT on synaptic transmission at COM and MDN terminals. For these experiments, we first blocked postsynaptic 1A (with 30 nM WAY100635) and 2A (with 500 nM MDL11939) receptors to eliminate target-specific postsynaptic effects of 5-HT (e.g., Avesar and Gulledge, 2012) that might influence somatically recorded EPSPs. In these baseline conditions, optical activation of COM afferents generated robust EPSPs that were of similar amplitudes in IT and ET target neurons (n = 17 IT-ET pairs; **Figure 4E**, **F**, **Table 6**). Bath application of 40 μM 5-HT moderately reduced optically evoked COM EPSP amplitudes in both target neuron subtypes (by ~60%, **Table 6**), but had only modest and highly variable impact on PPRs (**Figure 4F**, **Table 6**). Serotonergic suppression of COM EPSPs was marginally more robust in ET target neurons than in IT targets ($p = 0.057$, $d = 0.50$, for 5-HT effects on initial EPSPs; $p = 0.061$, $d = 0.49$ for effects on the second EPSP, when comparing across IT and ET target neurons), and was long-lasting; 5-HT effects did not reverse within a 15 minute wash (**Table 6**).

Serotonergic effects on MDN EPSPs were also modest (**Figure 4E**, **F**; **Table 6**), particularly in IT target neurons where MDN EPSPs were suppressed by only ~25% relative to the ~55% reduction of EPSP amplitudes in ET neurons (n = 8 IT-ET pairs; $p = 0.054$ and 0.004, $d = 0.82$ and 1.48, for first and second EPSPs, respectively, when comparing across target neuron subtypes; **Figure 4G**). For both afferents, serotonergic

effects were larger than observed in sham experiments that showed almost no change in EPSPs measured at a similar time point (see above and **Figure 4G**). Finally, 5-HT had relatively little impact on PPRs in both ET and IT target neurons (**Figure 4F**, **H**; **Table 6**). These data suggest that 5-HT, like ACh, may preferentially suppress synaptic transmission at COM afferents while leaving MDN transmission largely unaffected.

Neuromodulation of monosynaptic inputs to IT and ET neurons

The data described above suggest that both ACh and 5-HT preferentially suppress glutamatergic synaptic transmission at COM, relative to MDN, terminals in the PL cortex. However, activation of COM and MDN afferents may trigger polysynaptic transmission in the local cortical circuit that could contribute to the differential impact of ACh or 5-HT. For instance, since MDN-evoked responses in ET neurons are largely polysynaptic (**Figure 2**), neuromodulation of MDN EPSPs in ET neurons may reflect changes elsewhere in the local network, rather than at MDN terminals themselves.

To test whether ACh and/or 5-HT suppress monosynaptic transmission from COM and MDN afferents, we conducted additional experiments in the presence of 1 μM TTX and 100 μM 4-AP. Monosynaptic COM EPSPs were suppressed by ~80 ± 12%, with negligible changes in PPR (n = 6 IT and 4 ET neurons, not necessarily in pairs; **Figure 5A**, **B**; **Table 7**). Alternatively, when monosynaptic MDN inputs were activated, EPSPs were largely absent in ET neurons (n = 2) and those occurring in IT target neurons were relatively insensitive to ACh (n = 7; **Figure 5C**, **D**; **Table 7**). When comparing cholinergic modulation of monosynaptic COM- (all target neurons) and MDN- (IT targets only) evoked EPSPs, the effect of ACh on initial EPSP amplitude was ~7-fold greater for COM afferents (at -78 ± 10%) than for MDN afferents (-11 ± 15%; n = 17, $p < 0.001$, *d* =

2.02, when comparing across afferents). These data suggest that ACh preferentially suppresses glutamate release from COM synaptic terminals in the PL cortex. Afferent-specific neuromodulation of synaptic transmission also points to a presynaptic locus of cholinergic effects, as postsynaptic effects of ACh on synaptic transmission are expected to be largely independent of afferent input.

5-HT also suppressed monosynaptic COM EPSPs, albeit to a lesser extent than observed with ACh. In these experiments, which did not include blockers of 5-HT receptors in baseline conditions, addition of 40 μM 5-HT reduced monosynaptic COM EPSPs by ~40-45% (n = 7 IT and 7 ET neurons, not necessarily pairs; **Figure 6A**, **B**; **Table 7**), but failed to suppress monosynaptic MDN EPSPs in IT neurons (n = 11; **Figure 6C**, **D**; **Table 7**). 5-HT had a greater impact on COM afferents relative to MDN inputs (n = 25; p = 0.010, *d* = 1.39, when comparing the effects of 5-HT on first EPSP amplitude across afferents). For both COM and MDN afferents, application of ACh or 5-HT produced little change in PPRs (**Figures 5D, 6D**; **Table 7**). This likely reflects differences in presynaptic release probability that occur when synaptic transmission is triggered directly by ChR2, rather than with action potentials (see, for instance, Cruikshank et al., 2010), which likely contributes to the lower baseline PPRs measured in the presence of TTX and 4-AP (see also **Figure 2C**). Taken together, our results suggest that both ACh and 5-HT regulate monosynaptic glutamate release preferentially at COM terminals while having little impact on MDN synaptic transmission.

Concentration-dependent neuromodulation of COM input to IT and ET neurons

We next measured the modulatory effects of ACh and 5-HT on COM synaptic transmission across a range of transmitter concentrations. For these experiments,

recordings were made of COM-evoked EPSPs (2 flashes at 20 Hz at 15 s intervals) in IT and ET target neurons (not necessarily in pairs) in tissue exposed to sequentially increasing concentrations of modulatory transmitter. For cholinergic modulation, COM EPSPs were measured in two groups of neurons in baseline conditions, across three increasing concentrations of ACh applied for 7 minutes each, and after 15 minutes of wash.

The first group of neurons (n = 7 IT and 10 ET) was exposed sequentially to eserine alone, eserine with 500 nM ACh, and eserine with 20 μM ACh, followed by a 15 minute wash period (**Figure 7A**). The second group of neurons (n = 8 IT and 7 ET) experienced sequential applications of 1, 10, and 40 μM ACh, all in the presence of 10 μM eserine, before a 15 minute wash period (**Figure 7A**). Bath application of eserine alone was sufficient to reduce EPSP amplitudes (by an average of 39 ± 14% and 32 ± 3.3% for the first and second EPSPs; n = 17; $p < 0.001$, $d \geq 1.72$ for each), and increase PPRs slightly (by 13 ± 14%; $p = 0.002$, $d = 0.91$), suggesting an endogenous level of ACh in the absence of acetylcholinesterase that is sufficient to modulate synaptic transmission at COM afferents (**Figure 7B**). We found that increasing ACh concentrations progressively reduced EPSP amplitudes and increased PPRs, saturating at about 10 μM ACh in the presence of eserine with an 88 ± 7% reduction in the first EPSP (**Figure 7B**). Fitting a Hill equation to the mean responses for EPSP 1 across experimental conditions (**Figure 7A**, inset; see **Methods**) allowed us to estimate the endogenous (i.e., eserine-revealed) ACh concentration to be ~139 nM, and using that value we calculated the IC_{50} for cholinergic suppression of COM EPSPs to be 177 ± 15 nM (mean ± SD).

A similar set of experiments was conducted using increasing concentrations of 5-HT (in the absence of 5-HT receptor antagonists; **Figure 8**). For these experiments, group 1 neurons (n = 11 IT and 7 ET) experienced sequential applications of 100 nM, 500 nM and 2 μM 5-HT while group 2 neurons (n = 12 IT and 5 ET) experienced 10, 40, and 100 μM 5-HT (**Figure 8A**). Weak suppression of COM EPSPs was observed at 100 nM, the lowest dose tested, where the first and second EPSPs were reduced by 20 ± 13% and 17 ± 10%, respectively (n = 18), but was robust at 2 μM 5-HT, where the first and second EPSPs were reduced by 66 ± 21% and 64 ± 15%, respectively (**Figure 8B**). Fitting a Hill equation to the mean data for EPSP 1 across all concentrations indicated an IC_{50} of 216 ± 38 nM (**Figure 8A** inset).

Interestingly, at 40 μM 5-HT, serotonergic suppression of the first (-64 ± 22%) and second (-64 ± 19%) COM EPSPs was only slightly greater in magnitude than the effects of 40 μM 5-HT in the presence of antagonists for 1A and 2A receptors (-60 ± 16%; p = 0.218, *d* = 0.43 for suppression of the first EPSP, and -57 ± 16%; p = 0.073, *d* = 0.64 for the second EPSPs; see **Figure 4** and **Table 6**, above), suggesting that 1A and 2A receptors are not major contributors to serotonergic modulation of glutamate release at COM afferents.

Pharmacology of neuromodulation of COM afferents to IT and ET neurons

We next asked which receptor subtypes contribute to the regulation of synaptic transmission at COM terminals. Given that both ACh and 5-HT suppress, rather than enhance, COM transmission, we focused on testing the roles of the $G_{i/o}$-coupled metabotropic receptors that are most associated with inhibition of glutamate release in the cortex. In the case of ACh, metabotropic signaling is mediated by muscarinic ACh

receptors (mAChRs), and so we first tested their broad involvement using atropine (1 μM), a non-specific mAChR antagonist. In the presence of atropine, pairs of COM EPSPs optically evoked at 20 Hz were 9.9 ± 2.4 mV and 15.1 ± 2.6 mV in amplitude for first and second EPSPs, respectively, and exhibited a PPR of 1.57 ± 0.26 (n = 8; **Figure 9A**, **B**). The addition of 20 μM ACh for five minutes reduced the first and second EPSP amplitudes by ~10%, to 8.8 ± 2.2 mV and 13.5 ± 2.6 mV, respectively, but had minimal impact on PPR (1.55 ± 0.16; see **Figure 9B** for statistics). These modest effects were dramatically less than observed above in the absence of atropine (n = 8; **see Table 5**) for both the first (n = 16; $p < 0.001$, $d = 10.70$, comparing experiments with and without atropine) and second ($p < 0.001$, $d = 11.41$) EPSPs, and for PPRs ($p = 0.112$, $d = 0.90$), and suggest that cholinergic modulation of COM afferents relies primarily on mAChRs.

Among the five mAChR subtypes, $G_{i/o}$-coupled M2 and M4 receptors are most associated with presynaptic regulation of transmitter release. To evaluate their potential involvement in regulating COM afferents, we tested the impact of 1 μM ACh (with 10 μM eserine) on COM EPSPs in the presence of M2- or M4-preferring pharmacological agents (**Figure 9C**, **D**). We chose to test a 1 μM concentration because it delivers a near-maximal, but not saturating, inhibition of COM EPSPs (**see Figure 7**) that allowed for observation of bidirectional changes in cholinergic modulation of COM transmission. It also allowed us to compare the impact of pharmacological manipulations with results from 15 experiments in which 1 μM ACh was applied first in a series of ACh concentrations (-73 ± 12% and -65 ± 10% reductions of EPSPs 1 and 2, respectively, with an increase in PPR of 38 ± 36%; see **Figure 7**).

To preferentially block M2 receptors, we applied AF-DX116 (5 μM; n = 8) for seven minutes prior to addition of 1 μM ACh. In the presence of the M2 antagonist, ACh reduced the first and second EPSPs by 31 ± 7 and 22 ± 10%, respectively, and increased PPR by 13 ± 9% (see **Figure 9D** for statistics). These changes were substantially less than those observed in control neurons exposed to 1 μM ACh in the absence of antagonist (**Figure 9E**). However, preferential blockade of M4 receptors with VU6028418 (5 μM; n = 15) limited the effects of ACh to an even greater extent, with first and second EPSPs being reduced by only 12 ± 12% and 12 ± 11%, respectively, with no net changes in PPRs (0 ± 12%; **Figure 9D**). Thus, in the presence of the M4 antagonist, ACh effects were far less than those observed with ACh alone or with ACh in the presence of the M2 antagonist (**Figure 9E**), and were similar to those observed in the presence of atropine (see **Figure 9A**; p = 0.701, *d* = 0.15, when comparing ACh-induced changes in first EPSP amplitude in atropine and in VU6028418). Finally, we found that the M4-selective positive allosteric modulator (PAM) VU0467154 (3 μM; n = 8) enhanced the suppressive effect of 1 μm ACh on COM EPSPs, with first and second EPSPs being reduced by 86 ± 8% and 85 ± 11%, respectively (**Figure 9D**, **E**). In the presence of the M4 PAM, ACh-induced changes in PPR were highly variable (+7 ± 50%), likely because some EPSPs were reduced to almost undetectable levels, leading to large and variable differences in first and second EPSP measurements trial-to-trial and across neurons. Taken together, these data point to M4 receptors as being key mediators of cholinergic suppression of COM afferents in the PL cortex.

Serotonergic inhibition of glutamatergic transmission in the forebrain is most associated with presynaptic 5-HT_{1B} (1B) type serotonin receptors (Tanaka and North,

1993; Rhoades et al., 1994; Laurent et al., 2002; Kjaerby et al., 2016; Rama, 2023). although 1A and 2A receptors have also been implicated (Troca-Marin and Geijo-Barrientos, 2010; Tian et al., 2017; Agahari and Stricker, 2021, 2025). The inclusion of 1A and 2A antagonists in our initial experiments (see **Figure 4**, **Table 6**) suggest that these receptors, that are otherwise prominent in the PL cortex (Amargos-Bosch et al., 2004), are not necessary for presynaptic regulation of glutamate release at COM terminals. To determine whether 1B receptors contribute to serotonergic modulation of COM afferents in the PL cortex, we compared the impact of 2 μM 5-HT on COM EPSPs in control experiments (n = 10) with the effect of 2 μM 5-HT in the presence of SB214461 (SB, 10 μM; n = 11), an antagonist with selectivity for 1B receptors (**Figure 10**). In control experiments, 2 μM 5-HT applied in the absence of any serotonergic antagonists reduced the first and second EPSPs, respectively, by 63 ± 10% and 51 ± 13%, and increased PPRs by 34 ± 30% (**Figure 10A**, **B**; **Table 8**). These effects were similar to those observed in our experiments above in which neurons experienced 2 μM 5-HT as part of a series of 5-HT concentrations (see **Figure 8**), where the first and second EPSPs were reduced by 63 ± 25% ($p = 0.931$, $d = 0.03$, when compared to control 2 μM 5-HT experiments) and 61 ± 19% ($p = 0.094$, $d = 0.60$), respectively, and PPRs were increased by +16 ± 33% ($p = 0.153$, $d = 0.57$).

In the presence of SB, the effect of 2 μM 5-HT was more modest, but remained potent in reducing the first (by 40 ± 14%) and second (by 38 ± 14%) EPSPs and generating a small increase in PPR (+5 ± 13%; **Figure 10A**, **B**; **Table 8**). When serotonergic effects were compared across control and SB conditions, the antagonist reduced, but did not block, serotonergic suppression of synaptic transmission (**Figure**

10C). The incomplete block of 5-HT effects by SB suggests that other 5-HT receptors may contribute to serotonergic suppression of COM afferents.

Modulation of COM afferents with presynaptic DREADD receptors

To directly assess the ability of presynaptic metabotropic receptors to modulate glutamate release from COM afferents, we expressed $G_{i/o}$- (hM4Di) or G_q- (hM3Dq) coupled DREADDs ("designer receptors exclusively activated by designer drugs") together with ChR2 unilaterally in the PL cortex (**Figure 11A**, **D**) and measured optically evoked EPSPs in contralateral IT and ET target neurons in baseline conditions and after adding the DREADD-specific agonist CNO (50 nM, 500 nM, or 5 μM).

With hM4Di co-expressed with ChR2, application of 5 μM CNO frequently resulted in large and sometimes complete inhibition of optically evoked EPSPs (**Figure 11C**) that did not wash out after many minutes. Still, as shown in simultaneous recordings of COM EPSPs in an IT-ET neuron pair (**Figure 11B**), results with 5 μM CNO could be variable even under identical experimental conditions. This likely reflects stochastic differences in hM4Di expression levels across presynaptic COM terminals. Because 5 μM CNO generated such long-lasting, and essentially irreversible effects, in some experiments we lowered the concentration of CNO to 500 or 50 nM to see if we could reverse CNO-induced effects during a 15 mixture wash (**Figure 11C**). However, across all CNO concentrations, effects on COM EPSPs were long-lasting and failed to reverse during experiments. When data for all CNO concentrations were combined (n = 14), CNO suppressed the first and second EPSPs by 72 ± 22% and 68 ± 21%, respectively, and increased PPR by 26 ± 32% (**Table 9**). These data confirm that presynaptic $G_{i/o}$-coupled receptors can be powerful modulators of synaptic transmission at COM afferents.

Finally, to test whether activation of presynaptic G_q receptors might modulate COM synaptic transmission, we co-expressed hM3Dq with ChR2 in COM afferents and measured optically evoked EPSPs in baseline conditions and after addition of CNO (**Figure 11D**, **E**). Unlike for the hM4Di-expressing afferents described above, CNO application at 5 μM had negligible impact on COM transmission (n = 8; **Figure 11E**, **F**; **Table 9**), with EPSP amplitudes (mean changes of -6 + 13% and -5 ± 6% for the first and second EPSPs, respectively) and PPRs (+3 ± 16%) being very similar to baseline values (**Table 9**). These data suggest that presynaptic expression of G_q-coupled receptors may have only limited impact at COM synapses.

Discussion

Previous studies have found that 5-HT and ACh differentially regulate the postsynaptic excitability of IT and ET neurons in the mouse cortex (Dembrow et al., 2010; Avesar and Gulledge, 2012; Stephens et al., 2014; Joshi et al., 2015; Baker et al., 2018), suggesting that these neuromodulators may shift the balance of cortical output toward corticostriatal circuits or deep brain structures, respectively. In the present study, we tested whether presynaptic regulation of excitatory synaptic transmission in the PL cortex is similarly afferent- and/or target-specific. As discussed below, our results confirm target-specific connectivity of MDN afferents but reveal qualitatively similar selective presynaptic modulation of COM terminals, with both neuromodulators preferentially gating (i.e., being permissive of) MDN inputs that selectively target IT neurons in layer 5 but that can otherwise drive local network activity, including in ET neurons.

Targeting of COM and MDN afferents

Consistent with several previous studies (Lee et al., 2014; Dembrow et al., 2015; Anastasiades et al., 2018; Leyrer-Jackson and Thomas, 2019; Yi et al., 2022), we found that optogenetic activation of COM afferents generated robust and roughly equivalent monosynaptic synaptic responses in IT and ET target neurons (see **Figures 1D, 2B**). We also found that COM synapses displayed largely target-independent short-term plasticity (paired-pulse facilitation) across a range of input frequencies (see **Figures 1E** and **3B**). This contrasts with earlier studies reporting that COM afferents exhibit paired-pulse facilitation in ET neurons but paired-pulse depression in IT neurons (Lee et al., 2014; Leyrer-Jackson and Thomas, 2019), less paired-pulse depression in ET neurons (Yi et al., 2022), or paired-pulse depression of similar magnitudes at unitary corticocortical connections involving presynaptic IT neurons (Morishima et al., 2011). The diversity of these prior results cannot easily be explained by differences in animal age or strain (adult C57 mice, except for Morishima et al.) or by differences in extracellular calcium concentrations, which were 2 mM (Lee et al.; Yi et al.) or lower (~ 1 mM; Morishima et al.; Leyrer-Jackson and Thomas), and which would otherwise promote facilitating synaptic responses. Interestingly, all of these previous studies used 10 Hz stimulation to calculate PPR, which we found to generate less facilitation than EPSPs driven at 20 or 40 Hz (see Figure 3B and Martinetti et al., 2022), and employed shorter inter-trial intervals (8-10 s) than used in our experiments (15 s). These differences in experimental approach may contribute to the diversity of prior findings, as Burke et al. (2018) observed in layer 5 of mPFC a paired-pulse facilitation of similar magnitude to our study (PPR of ~1.5) for a range of afferent input, including COM

EPSPs and unitary events, with 20 Hz stimulation delivered at 15 s intervals. Our data go further in showing that, under our experimental conditions, short-term synaptic plasticity of COM afferents is largely target-independent across the range of 10 to 40 Hz.

We found thalamocortical projections from the MDN to be highly selective for IT target neurons in the PL cortex. This result is broadly consistent with Collins et al. (2018), who also observed a strong bias for monosynaptic connections in IT target neurons in layer 5 of the PL cortex. However, unlike Collins et al., who reported paired-pulse depression of MDN inputs to layer 2/3 pyramidal neurons at 10 Hz, we observed facilitation in layer 5 IT neurons across the range of 10, 20, and 40 Hz (see **Figure 3B**). This might reflect target-neuron-dependent differences in short-term plasticity, as Collins et al. did not report PPR in layer 5 IT neurons, but more likely results from subtile differences in experimental approach (see above). Overall, our data suggest that, whereas COM afferents robustly target both IT and ET neurons in layer 5 with similar synaptic dynamics, MDN afferents selectively innervate IT target neurons, but can indirectly excite ET neurons via IT-driven network activity (see also Collins et al., 2018).

Afferent-selective neuromodulation of excitatory drive

Given that ACh and 5-HT reciprocally regulate the postsynaptic excitability of two distinct cortical output channels (IT and ET neurons), we tested whether these neuromodulators might also differentially regulate excitatory synaptic drive in IT and ET neurons, perhaps in an afferent- and/or target-specific manner. Our main result is that both ACh and 5-HT suppressed glutamate release selectively at COM afferents in both

target neuron subtypes, albeit to different degrees, while having little impact on monosynaptic MDN transmission.

Afferent-specific cholinergic modulation of glutamate release has been widely reported for excitatory transmission in the neocortex (Gil et al., 1997; Hsieh et al., 2000), hippocampus (Kahle and Cotman, 1989; Hasselmo and Schnell, 1994; Kremin and Hasselmo, 2007), olfactory tubercle (Owen and Halliwell, 2001), piriform cortex (Hasselmo and Bower, 1992; Linster et al., 1999), and amygdala (Tryon et al., 2023). These studies, and our present results, are generally consistent with the hypotheses is that ACh presynaptically suppresses local network activity while being permissive for, or even amplifying, long-range afferent input (for review, see Giocomo and Hasselmo, 2007). While less studied, afferent-specific serotonergic suppression of transmission has been described for COM, relative to MDN, inputs to layer 5 neurons in PL cortex, albeit without identifying target neuron subtypes (Kjaerby et al., 2016). Conversely, in the nucleus accumbens, 5-HT was reported to selectively suppress thalamic inputs but not afferents from the mPFC (Christoffel et al., 2021). This suggests that presynaptic 5-HT receptor expression may be limited to a subpopulation of IT neurons in the mPFC (see below).

We found cholinergic suppression of COM transmission in the PL cortex to be almost absolute (>85%), suggesting that the majority of COM terminals express M4 receptors. Serotonergic modulation of COM EPSPs was less robust (~55% reduction at 40 μM 5-HT; see also Kjaerby et al., 2016) and more variable (SDs of 18% and 6%, for 5-HT and ACh, respectively). Even more modest effects of 5-HT (~25% reduction) were reported for electrically evoked (but putative COM) EPSPs in a subset of pyramidal

neurons in the anterior cingulate cortex (Troca-Marin and Geijo-Barrientos, 2010; see also Tian et al., 2017).

The finding that ACh strongly suppresses glutamatergic transmission, while 5-HT effects are more moderate at the same synapses, appears to be conserved across many of the studies listed above. For instance, in the olfactory tubercle ACH and 5-HT exhibit afferent-specific presynaptic regulation of glutamate release at local associational synapses, where the suppressive effect of ACh (~70%) is much greater than for serotonergic effects (~30%) and with ACh increasing PPR to a greater extent (~+60% vs ~+20%) than 5-HT (Owen and Halliwell, 2001; Hadley and Halliwell, 2010). Thus, there may be distinct presynaptic mechanisms that allow ACh and 5-HT to regulate synaptic transmission to different degrees. Alternatively, and consistent with the results of Christoffel et al. (2021; see above), it is possible that there is heterogeneity among the IT neurons that contribute to COM projections, with only a subset of neurons expressing presynaptic 5-HT receptors. There may also be heterogeneity in expression of presynaptic 5-HT receptors, as we found that 1B receptors to be only partially responsible for suppression of COM EPSPs, and consensus regarding which 5-HT receptor subtype(s) regulate glutamate release in the cortex is lacking.

Neuromodulation of COM afferents is presynaptic

Several observations suggest that ACh and 5-HT suppress COM transmission via presynaptic mechanisms. First, although it is possible (and expected) that postsynaptic changes in membrane excitability will impact postsynaptic potentials (e.g., by changing their electrotonic structure), such changes would be expected to have broadly similar effects on both COM and MDN EPSPs, as both afferents innervate similar dendritic

domains (Anastasiades and Carter, 2021). Secondly, cholinergic suppression of COM EPSPs was ascribed to M4 receptors, which are not associated with postsynaptic regulation of pyramidal neurons (Gulledge et al., 2009; Dasari and Gulledge, 2011), while serotonin reduced COM EPSPs approximately equally in the presence or absence of antagonists for the 1A and 2A receptors responsible for the opposing postsynaptic serotonergic effects in ET and IT neurons, respectively (Avesar and Gulledge, 2012; Stephens et al., 2014; Stephens et al., 2018); if 5-HT were influencing EPSP postsynaptically, we would expect target-specific, rather than afferent-specific, modulation of synaptic transmission. Thirdly, while 20 μM ACh reduced COM EPSPs in ET neurons by almost 90% (see **Table 5**), ACH induces an overall increase in spontaneous EPSP amplitude and frequency in ET neurons under the same experimental conditions (Gulledge, 2024). Finally, ACh across a range of concentrations increased paired-pulse facilitation, a classical, but not definitive (see Burke et al., 2018) indicator of presynaptic modulation of transmitter release.

While 5-HT did not greatly impact PPRs, the bulk of evidence above points to similar presynaptic mechanism for serotonergic regulation of COM EPSPs. In that light, an interesting parallel exists for pre- and postsynaptic dopaminergic modulation in the mPFC. Dopamine acting on dopamine D1 (G_s-coupled) receptors weakly excites IT neurons (Seong and Carter, 2012), while dopamine D2-type ($G_{i/o}$-coupled) receptor activation strongly enhances the gain of ET neurons (Gee et al., 2012). At the same time, presynaptic D1 receptors selectively suppress glutamate release at COM, but not MDN terminals (Burke et al., 2018). Interestingly, D1-mediated suppression of COM EPSPs (~40-50%; Burke et al., 2018) is similar in magnitude to serotonergic effects at

the same terminals (~60% reduction), and both forms of presynaptic modulation produced little, if any, changes in PPRs. Thus, 5-HT and dopamine may share a common mechanism for presynaptic modulation at COM terminals that is distinct from that engaged by ACh.

Functional implications

Although 5-HT and ACh both suppress excitatory transmission at COM terminals, the magnitude of suppression is much greater for ACh (~87% reduction; **Table 5**) than for 5-HT (~60% reduction; **Table 6**) at saturating concentrations for each modulator. Combined with target-specific postsynaptic regulation of IT and ET excitability, these data suggest that 5-HT and ACh may have different impact on information processing in cortical circuits. **Figure 12** presents a model for serotonergic and cholinergic regulation of PL cortex that incorporates both pre- and postsynaptic mechanisms in a subset of local and long-distance circuits. In this model, IT neurons innervate both IT and ET target neurons, while ET neurons selectively target other ET neurons (Morishima and Kawaguchi, 2006; Morishima et al., 2011; Kiritani et al., 2012). IT neurons also project bilaterally to the striatum with dense terminal ramifications, while ET neurons project only unilaterally and send fewer, more focused axon collaterals to the striatum (Zheng and Wilson, 2002; Hooks et al., 2018). Interestingly, recent connectivity mapping has found that the MDN and PL cortex project to similar striatal target zones in the dorsomedial stratum and nucleus accumbens (Hunnicutt et al., 2016), and that these stratal circuits, in turn, provide feedback to the MDN that may be net excitatory or inhibitory, depending on activity within striatal circuits (for review, see Groenewegen et al., 2016).

In this model, cortical release of 5-HT is expected to increase the gain of IT neurons (via postsynaptic 2A receptors), silence ET neurons (via postsynaptic 1A receptors), and reduce, but not eliminate, IT-mediated corticocortical transmission (**Figure 12B**). Therefore, 5-HT release in the cortex is expected to preferentially promote corticostriatal circuits driven primarily by thalamocortical projections (e.g., from MDN) that are not sensitive to presynaptic serotonergic regulation. The increased gain of IT neurons may compensate for the reduced corticocortical connectivity in networks of IT neurons to amplify, and perhaps widen, cortico-striatal-thalamic circuit activity.

Corticocortical transmission is more sensitive to cholinergic modulation (**Figure 12C**), which also preferentially enhances the the excitability of, and recurrent activity in, networks of ET neurons via postsynaptic M1 receptors (Gulledge et al., 2009; Baker et al., 2018; Gulledge, 2024). Given that a subpopulation of ET neurons monosynaptically excites thalamocortical neurons in the MDN (Collins et al., 2018), ACh release in the cortex may directly promote behavioral output (via brainstem projections) by driving focused, and perhaps narrowing, thalamocortical loops (**Figure 12C**) that have more balanced, and perhaps overlapping, contributions of ET and IT corticostriatal projections but strongly reduced intra-areal corticocortical communication (Shepherd and Yamawaki, 2021).

Although greatly oversimplified and omitting many neuron subtypes (including GABAergic interneurons) and synapses that may themselves be modulated by ACh and/or 5-HT, the model presented in **Figure 12** provides testable predictions about corticostriatal circuit behavior in the PL cortex *in vivo* across a variety of neuromodulatory conditions and pharmacological or chemogenetic interventions.

Bibliography

Agahari FA, Stricker C (2021) Serotonergic Modulation of Spontaneous and Evoked Transmitter Release in Layer II Pyramidal Cells of Rat Somatosensory Cortex. Cereb Cortex 31:1182-1200.

Agahari FA, Stricker C (2025) Modulation by serotonin reveals preferred recurrent excitatory connectivity in layer II of rat neocortex. Cereb Cortex 35.

Amargos-Bosch M, Bortolozzi A, Puig MV, Serrats J, Adell A, Celada P, Toth M, Mengod G, Artigas F (2004) Co-expression and*in vivo*interaction of serotonin1A and serotonin2A receptors in pyramidal neurons of prefrontal cortex. Cereb Cortex 14:281-299.

Anastasiades PG, Carter AG (2021) Circuit organization of the rodent medial prefrontal cortex. Trends Neurosci.

Anastasiades PG, Marlin JJ, Carter AG (2018) Cell-Type Specificity of Callosally Evoked Excitation and Feedforward Inhibition in the Prefrontal Cortex. Cell Rep 22:679-692.

Andrade R (1991) Cell excitation enhances muscarinic cholinergic responses in rat association cortex. Brain Research 548:81-93.

Araneda R, Andrade R (1991) 5-Hydroxytryptamine2 and 5-hydroxytryptamine 1A receptors mediate opposing responses on membrane excitability in rat association cortex. Neuroscience 40:399-412.

Athilingam JC, Ben-Shalom R, Keeshen CM, Sohal VS, Bender KJ (2017) Serotonin enhances excitability and gamma frequency temporal integration in mouse prefrontal fast-spiking interneurons. Elife 6.

Avesar D, Gulledge AT (2012) Selective serotonergic excitation of callosal projection neurons. Front Neural Circuits 6:12.

Baker AL, O'Toole RJ, Gulledge AT (2018) Preferential cholinergic excitation of corticopontine neurons. J Physiol 596:1659-1679.

Beaulieu-Laroche L, Harnett MT (2018) Dendritic Spines Prevent Synaptic Voltage Clamp. Neuron 97:75-82 e73.

Betke KM, Wells CA, Hamm HE (2012) GPCR mediated regulation of synaptic transmission. Prog Neurobiol 96:304-321.

Burke KJ, Jr., Keeshen CM, Bender KJ (2018) Two Forms of Synaptic Depression Produced by Differential Neuromodulation of Presynaptic Calcium Channels. Neuron 99:969-984 e967.

Christoffel DJ, Walsh JJ, Hoerbelt P, Heifets BD, Llorach P, Lopez RC, Ramakrishnan C, Deisseroth K, Malenka RC (2021) Selective filtering of excitatory inputs to nucleus accumbens by dopamine and serotonin. Proc Natl Acad Sci U S A 118.

Cohen J (1988) Statistical power analysis for the behavioral sciences, 2nd ed. Hillsdale, NJ: Lawrence Erlbaum Associates.

Colangelo C, Shichkova P, Keller D, Markram H, Ramaswamy S (2019) Cellular, Synaptic and Network Effects of Acetylcholine in the Neocortex. Front Neural Circuits 13:24.

Collins DP, Anastasiades PG, Marlin JJ, Carter AG (2018) Reciprocal Circuits Linking the Prefrontal Cortex with Dorsal and Ventral Thalamic Nuclei. Neuron 98:366-379 e364.

Cruikshank SJ, Urabe H, Nurmikko AV, Connors BW (2010) Pathway-specific feedforward circuits between thalamus and neocortex revealed by selective optical stimulation of axons. Neuron 65:230-245.

Dasari S, Gulledge AT (2011) M1 and M4 receptors modulate hippocampal pyramidal neurons. J Neurophysiol 105:779-792.

Dembrow NC, Chitwood RA, Johnston D (2010) Projection-specific neuromodulation of medial prefrontal cortex neurons. J Neurosci 30:16922-16937.

Dembrow NC, Zemelman BV, Johnston D (2015) Temporal dynamics of L5 dendrites in medial prefrontal cortex regulate integration versus coincidence detection of afferent inputs. J Neurosci 35:4501-4514.

Elliott MC, Tanaka PM, Schwark RW, Andrade R (2018) Serotonin Differentially Regulates L5 Pyramidal Cell Classes of the Medial Prefrontal Cortex in Rats and Mice. eNeuro 5.

Gee S, Ellwood I, Patel T, Luongo F, Deisseroth K, Sohal VS (2012) Synaptic activity unmasks dopamine D2 receptor modulation of a specific class of layer V pyramidal neurons in prefrontal cortex. J Neurosci 32:4959-4971.

Gil Z, Connors BW, Amitai Y (1997) Differential regulation of neocortical synapses by neuromodulators and activity. Neuron 19:679-686.

Giocomo LM, Hasselmo ME (2007) Neuromodulation by glutamate and acetylcholine can change circuit dynamics by regulating the relative influence of afferent input and excitatory feedback. Mol Neurobiol 36:184-200.

Groenewegen HJ, Voorn P, Scheel-Krüger J (2016) Limbic-Basal Ganglia Circuits Parallel and Integrative Aspects. In: The Basal Ganglia: Novel Perspectives on Motor and Cognitive Functions (Soghomonian J-J, ed), pp 11-45. Cham: Springer International Publishing.

Gulledge AT (2024) Cholinergic Activation of Corticofugal Circuits in the Adult Mouse Prefrontal Cortex. The Journal of Neuroscience 44:e1388232023.

Gulledge AT, Bucci DJ, Zhang SS, Matsui M, Yeh HH (2009) M1 receptors mediate cholinergic modulation of excitability in neocortical pyramidal neurons. J Neurosci 29:9888-9902.

Hadley JK, Halliwell JV (2010) Serotonin modulates glutamatergic transmission in the rat olfactory tubercle. Eur J Neurosci 31:659-672.

Hasselmo ME, Bower JM (1992) Cholinergic suppression specific to intrinsic not afferent fiber synapses in rat piriform (olfactory) cortex. J Neurophysiol 67:1222-1229.

Hasselmo ME, Schnell E (1994) Laminar selectivity of the cholinergic suppression of synaptic transmission in rat hippocampal region CA1: computational modeling and brain slice physiology. J Neurosci 14:3898-3914.

Hooks BM, Papale AE, Paletzki RF, Feroze MW, Eastwood BS, Couey JJ, Winnubst J, Chandrashekar J, Gerfen CR (2018) Topographic precision in sensory and motor corticostriatal projections varies across cell type and cortical area. Nat Commun 9:3549.

Hsieh CY, Cruikshank SJ, Metherate R (2000) Differential modulation of auditory thalamocortical and intracortical synaptic transmission by cholinergic agonist. Brain research 880:51-64.

Hunnicutt BJ, Jongbloets BC, Birdsong WT, Gertz KJ, Zhong H, Mao T (2016) A comprehensive excitatory input map of the striatum reveals novel functional organization. Elife 5.

Joshi A, Middleton JW, Anderson CT, Borges K, Suter BA, Shepherd GM, Tzounopoulos T (2015) Cell-specific activity-dependent fractionation of layer 2/3-->5B excitatory signaling in mouse auditory cortex. J Neurosci 35:3112-3123.

Kahle JS, Cotman CW (1989) Carbachol depresses synaptic responses in the medial but not the lateral perforant path. Brain research 482:159-163.

Kiritani T, Wickersham IR, Seung HS, Shepherd GM (2012) Hierarchical connectivity and connection-specific dynamics in the corticospinal-corticostriatal microcircuit in mouse motor cortex. J Neurosci 32:4992-5001.

Kjaerby C, Athilingam J, Robinson SE, Iafrati J, Sohal VS (2016) Serotonin 1B Receptors Regulate Prefrontal Function by Gating Callosal and Hippocampal Inputs. Cell Rep 17:2882-2890.

Kremin T, Hasselmo ME (2007) Cholinergic suppression of glutamatergic synaptic transmission in hippocampal region CA3 exhibits laminar selectivity: Implication for hippocampal network dynamics. Neuroscience 149:760-767.

Laurent A, Goaillard JM, Cases O, Lebrand C, Gaspar P, Ropert N (2002) Activity-dependent presynaptic effect of serotonin 1B receptors on the somatosensory thalamocortical transmission in neonatal mice. J Neurosci 22:886-900.

Lee AT, Gee SM, Vogt D, Patel T, Rubenstein JL, Sohal VS (2014) Pyramidal neurons in prefrontal cortex receive subtype-specific forms of excitation and inhibition. Neuron 81:61-68.

Leyrer-Jackson JM, Thomas MP (2019) Dopaminergic D1 receptor effects on commissural inputs targeting layer V pyramidal subtypes of the mouse medial prefrontal cortex. Physiol Rep 7:e14256.

Linster C, Wyble BP, Hasselmo ME (1999) Electrical stimulation of the horizontal limb of the diagonal band of broca modulates population EPSPs in piriform cortex. J Neurophysiol 81:2737-2742.

Martinetti LE, Bonekamp KE, Autio DM, Kim HH, Crandall SR (2022) Short-Term Facilitation of Long-Range Corticocortical Synapses Revealed by Selective Optical Stimulation. Cereb Cortex 32:1932-1949.

Morishima M, Kawaguchi Y (2006) Recurrent connection patterns of corticostriatal pyramidal cells in frontal cortex. J Neurosci 26:4394-4405.

Morishima M, Morita K, Kubota Y, Kawaguchi Y (2011) Highly Differentiated Projection-Specific Cortical Subnetworks. J Neurosci 31:10380-10391.

Murakoshi T, Song SY, Konishi S, Tanabe T (2001) Multiple G-protein-coupled receptors mediate presynaptic inhibition at single excitatory synapses in the rat visual cortex. Neurosci Lett 309:117-120.

Nieuwenhuis S, Forstmann BU, Wagenmakers EJ (2011) Erroneous analyses of interactions in neuroscience: a problem of significance. Nat Neurosci 14:1105-1107.

Oswald MJ, Tantirigama ML, Sonntag I, Hughes SM, Empson RM (2013) Diversity of layer 5 projection neurons in the mouse motor cortex. Front Cell Neurosci 7:174.

Owen GS, Halliwell JV (2001) Electrophysiological characterization of laminar synaptic inputs to the olfactory tubercle of the rat studied in vitro: modulation of glutamatergic transmission by cholinergic agents is pathway-specific. Eur J Neurosci 13:1767-1780.

Petreanu L, Huber D, Sobczyk A, Svoboda K (2007) Channelrhodopsin-2-assisted circuit mapping of long-range callosal projections. Nat Neurosci 10:663-668.

Petreanu L, Mao T, Sternson SM, Svoboda K (2009) The subcellular organization of neocortical excitatory connections. Nature 457:1142-1145.

Puig MV, Gulledge AT (2011) Serotonin and prefrontal cortex function: neurons, networks, and circuits. Mol Neurobiol 44:449-464.

Rama R (2023) Morphological and functional characterization of layer 5 neurons in rat medial prefrontal cortex, their synaptic microcircuitry and serotonin modulation. In: RWTH Aachen University, p 116. Jülich: RWTH Aachen University.

Rhoades RW, Bennett-Clarke CA, Shi MY, Mooney RD (1994) Effects of 5-HT on thalamocortical synaptic transmission in the developing rat. J Neurophysiol 72:2438-2450.

Schicker KW, Dorostkar MM, Boehm S (2008) Modulation of transmitter release via presynaptic ligand-gated ion channels. Curr Mol Pharmacol 1:106-129.

Seong HJ, Carter AG (2012) D1 receptor modulation of action potential firing in a subpopulation of layer 5 pyramidal neurons in the prefrontal cortex. J Neurosci 32:10516-10521.

Sheets PL, Suter BA, Kiritani T, Chan CS, Surmeier DJ, Shepherd GM (2011) Corticospinal-specific HCN expression in mouse motor cortex: I(h)-dependent synaptic integration as a candidate microcircuit mechanism involved in motor control. J Neurophysiol 106:2216-2231.

Shepherd GMG, Yamawaki N (2021) Untangling the cortico-thalamo-cortical loop: cellular pieces of a knotty circuit puzzle. Nat Rev Neurosci 22:389-406.

Stephens EK, Avesar D, Gulledge AT (2014) Activity-dependent serotonergic excitation of callosal projection neurons in the mouse prefrontal cortex. Frontiers in Neural Circuits 8.

Stephens EK, Baker AL, Gulledge AT (2018) Mechanisms Underlying Serotonergic Excitation of Callosal Projection Neurons in the Mouse Medial Prefrontal Cortex. Front Neural Circuits 12:2.

Tanaka E, North RA (1993) Actions of 5-hydroxytryptamine on neurons of the rat cingulate cortex. J Neurophysiol 69:1749-1757.

Tian Z, Yamanaka M, Bernabucci M, Zhao MG, Zhuo M (2017) Characterization of serotonin-induced inhibition of excitatory synaptic transmission in the anterior cingulate cortex. Mol Brain 10:21.

Troca-Marin JA, Geijo-Barrientos E (2010) Inhibition by 5-HT of the synaptic responses evoked by callosal fibers on cortical neurons in the mouse. Pflugers Arch 460:1073-1085.

Tryon SC, Bratsch-Prince JX, Warren JW, Jones GC, McDonald AJ, Mott DD (2023) Differential Regulation of Prelimbic and Thalamic Transmission to the Basolateral Amygdala by Acetylcholine Receptors. J Neurosci 43:722-735.

Tudi A, Yao M, Tang F, Zhou J, Li A, Gong H, Jiang T, Li X (2024) Subregion preference in the long-range connectome of pyramidal neurons in the medial prefrontal cortex. BMC Biol 22:95.

Vidal C, Changeux JP (1993) Nicotinic and muscarinic modulations of excitatory synaptic transmission in the rat prefrontal cortex in vitro. Neuroscience 56:23-32.

Wasserstein RL, Schirm AL, Lazar NA (2019) Moving to a World Beyond "$p < 0.05$". American Statistician 73:1-19.

Williams SR, Mitchell SJ (2008) Direct measurement of somatic voltage clamp errors in central neurons. Nat Neurosci 11:790-798.

Williams SR, Fletcher LN (2019) A Dendritic Substrate for the Cholinergic Control of Neocortical Output Neurons. Neuron 101:486-499 e484.

Yang D, Ding C, Qi G, Feldmeyer D (2021) Cholinergic and Adenosinergic Modulation of Synaptic Release. Neuroscience 456:114-130.

Yang D, Gunter R, Qi G, Radnikow G, Feldmeyer D (2020) Muscarinic and Nicotinic Modulation of Neocortical Layer 6A Synaptic Microcircuits Is Cooperative and Cell-Specific. Cereb Cortex 30:3528-3542.

Yi JH, Choe SY, Jung MW (2022) Variations in Commissural Input Processing Across Different Types of Cortical Projection Neurons. Cereb Cortex 32:2508-2520.

Zheng T, Wilson CJ (2002) Corticostriatal combinatorics: the implications of corticostriatal axonal arborizations. J Neurophysiol 87:1007-1017.

Additional information

Data availability
The authors agree to make all data available upon request.

Acknowledgments
We thank Saiko Ikeda for technical assistance with intracranial virus injections and data analysis, and Dartmouth undergraduate Ethan Liu for conducting experiments contributing to Figure 8.

Funding
This work was supported by a grant from the National Institute for Mental Health (R01 MH124934).

Conflicts of interest
The authors declare no competing financial interests.

Author contributions
ATG conceived of the project and contributed to experimental design, data acquisition, analysis, interpretation of data, and wrote and edited the manuscript. ALB contributed to experimental design, data acquisition, analysis, interpretation of data, and edited the manuscript.

Figure legends

Figure 1. Corticocortical and thalamocortical afferent input to IT and ET neurons in the prelimbic cortex. ***A***, Diagram (left) of approach for delivering ChR2-mCherry to commissural (COM) corticocortical (top) and thalamocortical (MDN; bottom) afferents to the prelimbic cortex, and images of injection sites (right). ***B***, Diagrams of experimental setup for recording light-triggered COM (top) or MDN (bottom) EPSPs in pairs of IT and ET neurons. ***C***, COM (top) and MDN (bottom) EPSPs (averages of 10 consecutive trials) recorded in pairs of IT (red traces) and ET (blue traces) layer 5 neurons in response to two flashes (1 ms) of blue light. ***D***, Comparison of the first EPSP amplitudes (left) and paired-pulse ratios (PPR; right) in pairs of IT (red) and ET (blue) target neurons. ***E***, Comparison of COM (top) and MDN (bottom) mean EPSP amplitudes in response to increasing LED power. The number of data points (neurons) falls off at higher light intensities as some neurons had only suprathreshold EPSPs. ***F***, Ten consecutive trials of COM (top) or MDN (bottom) synaptic activation (1 mW) recorded in pairs of IT (red) and ET (blue) neurons. The proportions (%) of trials exhibiting an AP for each flash are shown. ***G***, Plots of the mean probabilities of action potential (AP) generation (± SEM) across all trials and all IT and ET target neurons in response to increasing LED intensity for COM (top) and MDN (bottom) inputs. Numbers below bars indicate the number of IT (red) and ET (blue) neurons (out of the 18 or 16 neurons per group) that exhibited an AP in at least one trial at the given LED intensity.

Figure 2. Monosynaptic connectivity of callosal (COM) and thalamocortical (MDN) inputs to IT and ET neurons. ***A***, Average EPSPs (10 consecutive trials) in pairs of IT (red traces) and ET (blue traces) target neurons following activation of COM (upper traces) or MDN (lower traces) afferents in baseline conditions and after application of 1 μM TTX and 100 μM 4-AP at the indicated LED intensities. ***B***, Comparisons of first EPSP amplitudes in IT-ET pairs in baseline conditions and after isolation of monosynaptic inputs with TTX and 4-AP. Gray lines indicate individual neuron pairs, with the dashed lines indicating data for neurons shown in ***A***. Mean values and standard deviations are offset with filled symbols. P-values for Student's t-tests for paired data and effect sizes (Cohen's *d*) are shown. ***C***, Similar to ***B***, but for paired-pulse ratios. In some neurons, the second EPSP was suprathreshold in baseline conditions, leading to a reduction in the number of pairs quantified for PPR in baseline conditions.

Figure 3. Frequency-dependent short-term plasticity in commissural (COM) and corticothalamic (MDN) inputs to IT and ET neurons and response stability over time. ***A***, Ten consecutive responses (gray traces) and their averages (colored traces) to trains of 10 flashes delivered at 10 (left), 20 (middle), and 40 Hz (right) Hz in a IT-ET pair of target neurons experiencing COM input (top and middle traces) and in a different IT neuron experiencing activation of MDN inputs (lower traces). ***B***, Plots of mean normalized EPSP amplitudes (relative to 1st EPSP; ±SEM) during trains of ten optically evoked EPSPs from COM afferents onto IT and ET neurons (red and blue symbols, respectively; not all data from pairs) and from MDN afferents in IT neurons (purple symbols) at the indicated frequencies. ***C***, Ten consecutive trials (gray traces) and average responses (colored traces) in an IT-ET pair experiencing COM-evoked synaptic input under baseline conditions over a 30 minute period (left) and a summary plot of mean EPSP amplitudes over time (±SEM) for 6 IT and 6 ET neurons (not necessarily in pairs). ***D***, Similar to ***C***, but for optical activation of MDN inputs.

Figure 4. Cholinergic and serotonergic modulation of excitatory afferents in the prelimbic cortex. ***A***, Diagrams of approach for delivering ChR2-mCherry to commissural (COM; top) and thalamocortical (MDN; bottom) afferents to the prelimbic cortex. ***B***, Ten consecutive responses (grey) and their averaged responses (colored thick traces) in

pairs of IT (red) and ET (blue) target neurons following activation of COM (top) or MDN (bottom) afferents in baseline conditions (left), after application of 20 μM ACh (middle), and after 15-20 minutes of wash (right). ***C***, Comparisons of EPSP amplitudes (left, middle) and paired-pulse ratios (PPR; right) in IT (red) and ET (blue) target neurons in baseline conditions and in the presence of ACh. Dashed lines indicate data from traces shown in ***B***. Mean values and standard deviations are offset with filled symbols. P-values for Student's t-tests and effect sizes (Cohen's *d*) are color-coded to neuron subtype. ***D-F***, Similar to ***A-C***, but for application of 40 μM 5-HT. For 5-HT experiments, baseline conditions included WAY 100635 (30 nM) and MDL 11939 (500 nM) to block postsynaptic 5-HT receptors. Note that for MDN inputs, responses in ET neurons are largely polysynaptic (see main text). ***G-H***, Comparisons of treatment effects on first EPSP amplitudes and paired-pulse ratios for COM (***G***) and MDN (***H***) inputs to IT and ET neurons. Grey lines indicate means, and shaded areas denote standard deviations. The only large target-dependent effect was for serotonergic effects on MDN afferents (shown).

Figure 5. Selective cholinergic suppression of glutamate release from monosynaptic commissural (COM) afferents to IT and ET neurons in prelimbic cortex. ***A***, Ten consecutive optically activated COM EPSP pairs (grey traces) and their averaged responses (colored traces) in a pair of IT (red) and ET (blue) neurons in baseline conditions (left), after sequential and additive applications of 1 μM TTX, 100 μM 4-AP, and 20 μM ACh (with 10 μM eserine; middle traces), and after wash in TTX + 4-AP (right). ***B***, Plots of the effects of 20 μM ACh on COM EPSP amplitudes (left and middle) and paired-pulse ratios (PPR; right). ***C***, Ten consecutive responses (grey) and their averages (colored traces) for optical activation of thalamic (MDN) inputs to a pair of IT (red) and ET (blue) neurons. Note the lack of monosynaptic MDN input to the ET neuron. ***D***, Plots of the effects of 20 μM ACh on MDN EPSP amplitudes (left and middle) and paired-pulse ratios (PPR; right). P-values are for Student's t-tests for paired samples, while effect sizes are represented by Cohen's *d*, and are calculated from all neurons (for IT-only results for MDN inputs, see **Table 7**).

Figure 6. Selective serotonergic suppression of glutamate release from monosynaptic commissural (COM) afferents to IT and ET neurons in prelimbic cortex. ***A***, Ten consecutive optically activated COM EPSP pairs (grey traces) and their averaged responses (colored traces) in a pair of IT (red) and ET (blue) neurons in baseline conditions (left), after sequential and additive applications of 1 μM TTX, 100 μM 4-AP, and 40 μM 5-HT (middle traces), and after wash in TTX + 4-AP (right). ***B***, Plots of the effects of 40 μM 5-HT on COM EPSP amplitudes (left and middle) and paired-pulse ratios (PPR; right). ***C***, Ten consecutive EPSP traces (grey) and their averages (colored traces) for thalamic (MDN) inputs to a pair of IT (red) and ET (blue) neurons. ***D***, Plots of the effects of 40 μM 5-HT on MDN EPSP amplitudes (left and middle) and paired-pulse ratios (PPR; right). P-values are for Student's t-tests for paired samples, while effect sizes are represented by Cohen's *d*, and are calculated from all neurons (for IT-only results for MDN inputs, see ***Table 7***).

Figure 7. Dose-dependence of cholinergic suppression of excitatory transmission at commissural (COM) afferents. ***A***, Averages of ten consecutive light-evoked COM EPSPs (20 Hz; normalized to baseline EPSP amplitudes) in an IT neuron from "Group 1" and an ET neuron from "Group 2". After recording baseline COM EPSPs, IT and ET neurons in Group 1 received three consecutive treatments consisting of eserine alone (10 μM), eserine with 0.5 μM ACh, and eserine with 20 μM ACh, followed by 10 or more minutes of wash. Group 2 IT and ET neurons were exposed to eserine combined with three increasing doses of ACh (1, 10, and 40 μM). Each dose was applied for 7 minutes. Inset is a plot of normalized responses vs ACh concentrations fit with a Hill equation for raw data (solid green line) and after estimating the eserine-only concentration at 139 nM (orange data point and dashed green line). ***B***, Plots of EPSP amplitudes (top two graphs) and paired-pulse ratios (bottom graph) for each neuron in the various drug conditions (as measured from averages of final 10 responses per condition) for IT (red) and ET (blue) neurons in group 1 (open symbols) and Group 2 (closed symbols). Mean response amplitudes and standard deviations for each condition indicated by larger symbols to the left (IT; red) and right (ET; blue) of each condition. P-values and Cohen's d for each drug condition are relative to baseline measurements for the given group. Neurons not necessarily recorded in pairs.

Figure 8. Dose-dependence of serotonergic suppression of excitatory transmission at commissural (COM) afferents. ***A***, Averages of ten consecutive light-evoked COM EPSPs (20 Hz; normalized to baseline EPSP amplitudes) in two IT neurons (one from "Group 1" and one from "Group 2"). After recording baseline COM EPSPs, IT and ET neurons in Group 1 received three consecutively increasing doses of 5-HT (100 nM, 500 nM, and 2 μM) followed by 10 or more minutes of wash in the absence of drugs. Group 2 IT and ET neurons were consecutively exposed to 10, 40, and 100 μM 5-HT, before a similar wash. Inset is a plot of normalized responses vs 5-HT concentration fit with a Hill equation. ***B***, Plots of EPSP amplitudes (top two graphs) and paired-pulse ratios (bottom graph) for each neuron in the various drug conditions (as measured from the averages of ten consecutive trials per condition) for IT (red) and ET (blue) neurons in group 1 (open symbols) and Group 2 (closed symbols). Mean response amplitudes and standard deviations for each condition indicated by larger symbols to the left (IT; red) and right (ET; blue). Data from one Group 2 neuron with PPR values above 4 (4.8, 9.5, 4.6, and 6.4, respectively, for 10 μM, 40 μM, 100 μM, and wash) were excluded for calculations of mean and standard deviation and are not shown in plot. An additional pair of group 2 neurons was not exposed to 40 μM 5-HT. P-values and Cohen's d for each drug condition are relative to baseline measurements for the given group. Neurons were not necessarily recorded in pairs.

Figure 9. M4 muscarinic receptors mediate cholinergic suppression of commissural (COM) synaptic transmission. ***A***, Ten consecutive responses to optical activation of COM afferents (two 1-ms flashes at 20 Hz; grey traces) and averaged responses (blue

traces) in an ET neuron in the presence of 20 μM atropine (a non-specific muscarinic receptor blocker; left) and after addition of 20 μM ACh (with 10 μM eserine; right). ***B***, Summary plots of EPSP amplitudes (left and middle) and paired-pulse ratios (PPR; right) in baseline conditions with atropine present and after addition of ACh for eight neurons. Individual neurons shown with lines, with means and standard deviations for the different conditions offset. Dashed lines indicate data from neuron shown in ***A***. ***C***, Ten consecutive COM responses (grey) and averaged responses (colored traces) in IT (red) or ET (blue) neurons in various baseline conditions (as indicated; left) and after addition of 1 μM ACh (with 10 μM eserine; right). The top trace shows control experiments conducted in regular aCSF, while the other neurons were pre-exposed to M2- or M4-specific antagonists (middle traces) or an M4-specific positive allosteric modulator (PAM; lower traces), as indicated. ***D***, Plots of the effects of 1 μM ACh with eserine on COM EPSP amplitudes (top and middle) and paired-pulse ratios (PPR; bottom) for the different experimental conditions. Dashed lines indicate results from the neurons shown in ***C***. ***E***, Plots of the normalized first EPSP amplitudes (relative to baseline EPSPs; left) and PPR (right) in the presence of ACh for the different experimental conditions. Grey lines show means, grey shaded areas indicate standard deviations. P-values (Student's t tests) and effect sizes (Cohen's *d*) are indicated.

Figure 10. Contribution of 5-HT1B (1B) receptors to serotonergic modulation of commissural (COM) synaptic transmission. ***A***, Ten consecutive responses to optical activation of COM afferents (two 1-ms flashes at 20 Hz; grey traces) and averaged responses (red traces) in two IT neurons in baseline conditions (left) and after addition of 2 μM serotonin (5-HT; right) in control conditions (top neuron) and in the continued presence of 10 μM SB216641 (a 1B antagonist; bottom neuron). ***B***, Summary plots of EPSP amplitudes (left and middle) and paired-pulse ratios (PPR; right) in baseline conditions and in the presence of 5-HT. Individual neurons shown with lines, with means and standard deviations for the different conditions offset. Dashed lines indicate data from neurons shown in ***A***. ***C***, Plots of the normalized first EPSP amplitudes (relative to baseline EPSPs; left and middle) and PPR (right) in the presence of 5-HT for control neurons and those exposed to SB214461. Grey lines show means, grey shaded areas indicate standard deviations. P-values (Student's t tests) and effect sizes (Cohen's *d*) are indicated.

Figure 11. Activation of selectively expressed $G_{i/o}$, but not G_q, presynaptic metabotropic receptors suppresses commissural (COM) synaptic transmission. ***A***, Diagram of experimental setup, with AAV-induced co-expression of channelrhodopsin-2 (ChR2) and hM4Di ($G_{i/o}$-coupled) receptors in one cerebral hemisphere and subsequent optical activation of COM afferents in the opposite hemisphere before and after the application of clozapine-N-oxide (CNO). ***B***, Ten consecutive responses to pairs (20 Hz) of COM afferent activations (grey traces) and their averaged responses (colored traces) in a pair of IT (red) and ET (blue) neurons in baseline conditions (left) and after addition of 5 μM CNO (right). ***C***, Comparisons of EPSP amplitudes (left and middle) and paired-pulse ratios (PPR; right) before and after CNO applications at the noted concentrations for 14

neurons. Mean responses (± SD) shown with offset symbols. P-values (Student's t-tests for paired data) and effect sizes (Cohen's d) shown for each. Asterisks indicate data from panel ***B***. ***D***-***F***, Similar to ***A***-***C***, but for co-expression of ChR2 and hM3Dq, a G_q-coupled receptor for CNO. In panel ***F***, dashed lines indicate data from experiments shown in panel ***E***.

Figure 12. Circuit-level impact of 5-HT and ACh release in the prefrontal cortex. ***A***, Diagram of local and long-distance circuits subserved by IT (red) and ET (blue) neurons in the prefrontal cortex (PFC). IT neurons project bilaterally within the cortex and to the striatum (specifically the dorsomedial striatum and nucleus accumbens), while networks of interconnected ET neurons project ipsilaterally within the cortex, moderately to the striatum, and to one or more subcortical targets (e.g., the brainstem and/or the mediodorsal nucleus [MDN] of the thalamus). The MDN is bidirectionally connected with the striatum (projecting direct efferents and receiving feedback via the pallidum) and with the cortex (selectively targeting IT neurons in the PFC and receiving feedback via ET projections and striatal circuits). Green traffic lights indicate normal synaptic transmission in the absence of neuromodulation. ***B***, 5-HT increases the gain of IT neurons via 2A receptors and strongly inhibits ET neurons via 1A receptors, while moderately suppressing IT-derived corticocortical communication (yellow traffic symbols), perhaps via presynaptic 1B receptors. The net effect is preferential amplification of thalamocortically driven corticostriatal output bilaterally, which in turn may provide feedback to the MDN via the pallidum. ***C***, In the presence of ACh, M4 receptors strongly suppress IT-derived corticocortical communication (red traffic lights) while M1 receptors preferentially enhance the gain of interconnected ET neurons, promoting corticofugal output to the ipsilateral striatum and deep structures, including the MDN, which in turn promotes bilateral corticostriatal output via IT neurons.

Tables

Table1. AAV manipulations of prelimbic afferents

Target afferent	Hemisphere (relative to recording site)	Coordinates	Addgene #	Virus	Dilution	volume (nL)
Commissural (COM)	contralateral	lateral: ±0.48 rostral-caudal: +2.10 depth: -1.60	100054	pAAV.CAG.hChR2(H134R)-mCherry.WPRE.SV40	1:10 (*1:5)	300 (*150)
			50475	pAAV-hSyn-hM4D(Gi)-mCherry	1:5	250
			50474	pAAV-hSyn-hM3D(Gq)-mCherry	1:5	250
Mediodorsal nucleus (MDN)	ipsilateral	lateral: ±0.70 rostral-caudal: -1.48 depth: -3.30	100054	pAAV.CAG.hChR2(H134R)-mCherry.WPRE.SV40	1:10	300

All coordinates are relative to bregma. AAVs were of the AAV9 serotype. *When ChR2 was co-expressed with hM4Di or hM3Dq in COM afferents, dilution and concentration were reduced by half.

Table 2. Physiological classification of IT and ET neurons in prelimbic cortex

Neuron subtype	n	Age (days)	V_M (mV)	R_N (MΩ)	Sag (%)	Slope of sag (mV/ms)	Physiology index
IT	187	86 ± 33	-83.4 ± 6.0	121 ± 47	7.0 ± 4.8	8.4 ± 7.1	0.7 ± 0.9
ET	180	86 ± 32	-78.0 ± 3.0	51 ± 15	19.1 ± 7.9	53.5 ± 18.2	22.9 ± 15.0
IT vs ET	p-value	0.965	<0.001				
	Cohen's *d*	<0.01	1.13				

Physiological properties of neurons classified as IT or ET shown as means ± standard deviations. V_M is the resting membrane potential, R_N is the input resistance, sag and slope of sag are measures of HCN-channel mediated rebound from peak hyperpolarizations (see Methods). *P*-values are for Student's t-tests for paired samples, while effect sizes are represented by Cohen's *d*. Statistical comparisons were not made of metrics that were used to define neuron subtypes (see Methods).

Table 3. Properties of afferent inputs to pairs of IT and ET neurons in the prelimbic cortex

Afferent (# of pairs)	**Target neuron subtype**		**EPSP 1**			**EPSP 2**			**PPR**
			Amplitude (mV)	**Onset latency** (ms)	**half-width** (ms)	**Amplitude** (mV)	**Onset latency** (ms)	**half-width** (ms)	
COM (99)		IT	10.4 ± 4.2	1.88 ± 0.41	21 ± 8	15.6 ± 6.4	1.79 ± 0.41	25 ± 11	1.52 ± 0.36
		ET	9.0 ± 4.0	1.89 ± 0.40	14 ± 4	13.6 ± 5.9	1.89 ± 0.37	16 ± 5	1.56 ± 0.41
	IT vs ET	p-value	0.019	0.685	< 0.001	0.011	< 0.001	< 0.001	0.335
		Cohen's *d*	0.24	0.04	0.91	0.26	0.40	0.99	0.10
MDN (58)		IT	15.6 ± 8.4	1.98 ± 0.54	27 ± 10	21.3 ± 10.0	1.96 ± 0.53	28 ± 12	1.44 ± 0.41
		ET	6.4 ± 3.9	3.03 ± 1.33	20 + 7	11.4 ± 6.4	2.97 ± 1.12	23 ± 8	1.94 ± 0.86
	IT vs ET	p-value	< 0.001	< 0.001	< 0.001	< 0.001	< 0.001	< 0.001	< 0.001
		Cohen's *d*	0.94	0.83	0.69	0.86	0.82	0.49	0.63

Measurements of optically triggered EPSPs presented as means ± standard deviations.EPSP amplitudes measured relative to the mean V_M over the 50 ms prior to the first flash of light. Latencies measured as the point at which the EPSP reaches 5% of the peak value relative to the baseline V_M. EPSP "half-widths" were measured at half amplitude relative to the baseline V_M. *P*-values are for Student's t-tests for paired samples. Effect sizes are represented by Cohen's *d*.

Table 4. Monosynaptic targeting of IT and ET neurons

Afferent	Target neuron subtype		Baseline conditions			in TTX and 4-AP (increased LED)			ΔPPR p-value, Cohen's *d*
			EPSP 1 amplitude (mV)	**EPSP 2 amplitude** (mV)	**PPR**	**EPSP 1 amplitude** (mV)	**EPSP 2 amplitude** (mV)	**PPR**	
COM		n =	11 pairs	8 pairs*	8 pairs*	11 pairs	11 pairs	11 pairs	8 pairs*
		IT	11.8 ± 4.6	17.8 ± 6.2	1.57 ± 0.28	13.8 ± 6.9	16.6 ± 8.8	1.22 ± 0.25	0.002, 1.43
		ET	11.0 ± 3.4	15.8 ± 4.3	1.44 ± 0.24	9.2 ± 4.0	10.0 ± 5.4	1.08 ± 0.26	0.007, 1.12
	IT vs ET	p-value	0.713	0.417	0.375	0.069	0.014	0.118	
		Cohen's *d*	0.11	0.30	0.34	0.57	0.81	0.40	
MDN		n =	9 pairs	7 pairs	7 pairs	9 pairs	9 pairs	9 pairs	
		IT	15.3 ± 7.0	18.1 ± 5.3	1.52 ± 0.41	11.6 ± 3.8	14.0 ± 10.1	1.14 ± 0.59	0.096, 0.75
		ET	4.1 ± 2.4	7.1 ± 3.6	2.06 ± 1.16	1.4 ± 1.4	1.0 ± 1.0	0.94 ± 0.47	0.015, 1.28
	IT vs ET	p-value	0.003	0.002	0.306	<0.001	0.006	0.026	
		Cohen's *d*	1.37	1.96	0.42	2.08	1.23	0.91	

Measurements of optically triggered EPSPs presented as means ± standard deviations.EPSP amplitudes measured relative to the mean V_M over the 50 ms prior to the first flash of light. Latencies measured as the point at which the EPSP reaches 5% of the peak value relative to the baseline V_M. EPSP "half-widths" were measured at half amplitude relative to the baseline V_M. *P*-values are for Student's t-tests for paired samples. Effect sizes are represented by Cohen's *d*. *In baseline conditions, some neurons tested had 2nd EPSPs that were suprathreshold, and data are shown only for the remaining 8 pairs that had consistent subthreshold responses for both EPSPs.

Table 5. Cholinergic neuromodulation of COM and MDN afferents to IT and ET neurons

Afferent and Target neuron subtype	**Measurement**	**Baseline**	**+20 μM ACh (with eserine)**	**Wash**	**Change in ACh (%)**	ACh effect	
						t-test (p value)	**Effect size** (Cohen's *d*)
COM - IT (n = 8 pairs)	EPSP 1 amplitude (mV)	8.3 ± 2.6	1.1 ± 0.4	5. 0 ± 3.0	-86 ± 6	< 0.001	2.88
	EPSP 2 amplitude (mV)	10.3 ± 2.5	1.7 ± 0.5	7.4 ± 3.4	-84 ± 4	< 0.001	3.90
	PPR	1.27 ± 0.17	1.65 ± 0.68	1.56 ± 0.31	+29 ± 44	0.119	0.63
COM - ET	EPSP 1 amplitude (mV)	7.6 ± 3.3	0.8 ± 0.4	3.9 ± 2.1	-88 ± 8	< 0.001	2.92
	EPSP 2 amplitude (mV)	11.9 ± 4.5	1.7 ± 0.7	7.8 ± 4.3	-85 ± 6	< 0.001	3.20
	PPR	1.61 ± 0.32	2.27 ± 0.85	2.06 ± 0.57	+47 ± 64	0.096	1.03
MDN - IT (n = 13 pairs)	EPSP 1 amplitude (mV)	8.1 ± 2.8	6.4 ± 3.4	7.7 ± 3.4	-23 ± 25	0.015	0.56
	EPSP 2 amplitude (mV)	12.1 ± 5.1	8.3 ± 3.7	11.1 ± 5. 1	-29 ± 22	0.005	0.84
	PPR	1.48 ± 0.33	1.39 ± 0.37	1.45 ± 0.36	-6 ± 13	0.148	0.26
MDN -ET	EPSP 1 amplitude (mV)	2.6 ± 2.8	1.2 ± 0.9	1.9 ± 2.1	-24 ± 43	0.028	0.69
	EPSP 2 amplitude (mV)	3.7 ± 3.3	1.7 ± 1.2	3.0 ± 2.3	-37 ± 30	0.012	0.83
	PPR	2.18 ± 1.91	1.52 ± 0.73	2.85 ± 2. 38	-6 ± 30	0.133	0.45

Measurements of EPSP amplitudes are from the average of 10 consecutive trials in each experimental condition recorded in pairs of IT and ET target neurons. P-values are for Student's t-tests for paired samples comparing EPSP amplitudes in baseline and acetylcholine (ACh) conditions. Effect sizes for ACh effects are represented by Cohen's *d*.

Table 6. Serotonergic neuromodulation of COM and MDN afferents to IT and ET neurons

Afferent and Target neuron subtype (n)	**Measurement**	**Baseline** (MDL+WAY)	**+40 μM 5-HT**	**Wash**	**Change in 5-HT (%)**	5-HT effect	
						t-test (p value)	**Effect size** (Cohen's *d*)
COM - IT (n = 17 pairs)	EPSP 1 amplitude (mV)	7.7 ± 3.8	3.5 ± 2.2	4.6 ± 3. 7	-55 ± 18	< 0.001	1.37
	EPSP 2 amplitude (mV)	9.2 ± 5.0	4.6 ± 3.3	5.2 ± 4.3	-52 ± 18	< 0.001	1.07
	PPR	1.22 ± 0.32	1.35 ± 0.45	1.18 ± 0.43	+9 ± 18	0.016	0.34
COM - ET	EPSP 1 amplitude (mV)	6.7 ± 2.5	2.5 ± 1.5	3.0 ± 1.6	-65 ± 13	< 0.001	2.07
	EPSP 2 amplitude (mV)	9.3 ± 4.0	3.7 ± 2.7	4.7 ± 2.8	-61 ± 14	< 0.001	1.66
	PPR	1.41 ± 0.50	1.61 ± 0.82	1.70 ± 0.98	+12 ± 18	0.056	0.30
MDN - IT (n = 8 pairs)	EPSP 1 amplitude (mV)	9.8 ± 3.3	8.1 ± 3.4	7.7 ± 3.4	-26 ± 22	0.040	0.52
	EPSP 2 amplitude (mV)	15.1 ± 6.3	12.1 ± 5.1	11.1 ± 5. 1	-27 ± 19	0.050	0.51
	PPR	1.54 ± 0.35	0.83 ± 0.04	1.45 ± 0.36	+0.3 ± 17	0.826	0.04
MDN -ET	EPSP 1 amplitude (mV)	5.5 ± 3.7	3.0 ± 1.7	5.1 ± 1.9	-53 ± 27	0.124	0.85
	EPSP 2 amplitude (mV)	12.0 ± 5.7	6.3 ± 3.0	10.6 ± 4.5	-57 ± 19	0.008	1.25
	PPR	2.34 ± 0.99	2.10 ± 0.68	2.08 ± 0.86	+8 ± 67	0.438	0.29

Measurements of EPSP amplitudes are from the average of 10 consecutive trials in each experimental condition recorded in pairs of IT and ET target neurons. Baseline conditions included antagonists for 5-HT_{1A} (30 nM WAY100635) and 5-HT_{2A} (500 nM MDL11939) receptors to limit postsynaptic effects of 5-HT. P-values are for Student's t-tests for paired samples comparing EPSP amplitudes in baseline and serotonin (5-HT) conditions. Effect sizes for 5-HT effects are represented by Cohen's *d*.

Table 7. Neuromodulation of monosynaptic transmission in IT and ET target neurons

Afferent	**Measure**	**Baseline** (TTX+4-AP)	**+ACh**	**Wash**	**% Change in ACh**	**t-test** (p value)	**Effect size** (Cohen's *d*)
COM (n = 10)	EPSP 1 amplitude	10.5 ± 4.5	2.6 ± 2.0	8.0 ± 4.5	-78 ± 10	< 0.001	2.17
	EPSP 2 amplitude	14.8 ± 12.1	4.1 ± 4.2	10.3 ± 9.1	-77 ± 13	0.002	1.13
	PPR	1.35 ± 0.64	1.45 ± 0.75	1.23 ± 0.71	+7 ± 36	0.402	0.12
MDN (n = 7, IT only)	EPSP 1 amplitude	9.8 ± 3.8	8.6 ± 2.9	11.4 ± 3.9	-11 ± 15	0.043	0.38
	EPSP 2 amplitude	8.5 ± 4.2	7.7 ± 4.3	10.2 ± 5.8	-7 ± 23	0.359	0.18
	PPR	0.87 ± 0.25	0.91 ± 0.30	0.86 ± 0.25	+4 ± 20	0.558	0.15
Afferent	**Measure**	**Baseline** (TTX+4-AP)	**+5-HT**	**Wash**	**% Change in 5-HT**	**t-test** (P value)	**Effect size** (Cohen's *d*)
COM (n = 14)	EPSP 1 amplitude	10.5 ± 3.4	6.1 ± 2.8	5.5 ± 3.4	-44 ± 16	< 0.001	1.41
	EPSP 2 amplitude	11.7 ± 4.5	7.1 ± 3.6	7.2 ± 4.5	-41 ± 19	0.002	1.13
	PPR	1.13 ± 0.32	1.19 ± 0.44	1.27 ± 0.39	+4 ± 25	0.464	0.15
MDN (n = 11, IT only)	EPSP 1 amplitude	11.6 ± 4.1	13.7 ± 9.9	4.6 ± 2.9	+12 ± 58	0.391	0.29
	EPSP 2 amplitude	14.1 ± 8.8	13.3 ± 8.9	6.5 ± 4.0	-7 ± 35	0.622	0.09
	PPR	1.18 ± .0.55	0.99 ± 0.37	1.50 ± 0.40	-9 ± 26	0.296	0.40

Mean EPSP amplitudes and paired-pulse ratios (PPR; ± SD) of isolated monosynaptic commissural (COM) and thalamocortical (MDN) afferents under different experimental conditions. For COM afferents, IT and ET targets were combined. For MDN inputs, data are presented from IT targets only. Baseline EPSPs were generated in the presence of 1 μM TTX and 100 μM 4-AP and measurements in each condition are from the average of 10 consecutive trials. P-values are for Student's t-tests for paired samples, while effect sizes are represented by Cohen's *d*.

Table 8. Impact of 5-HT1B blockade on serotonergic suppression of COM afferents

Drug condition	Measure	Baseline	+2 μM 5-HT	Wash	% Change in 5-HT	t-test (p value)	Effect size (Cohen's *d*)
Control (n = 10)	EPSP 1 amplitude (mV)	10.0 ± 2.1	3.6 ± 0.9	8.5 ± 2.5	-63 ± 10	< 0.001	3.05
	EPSP 2 amplitude (mV)	15.6 ± 3.6	7.6 ± 2.1	13.7 ± 4.3	-51 ± 13	< 0.001	2.74
	PPR	1.57 ± 0.18	2.08 ± 0.38	1.61 ± 0.23	+34 ± 30	< 0.001	1.23
10 μM SB214461 (n = 11)	EPSP 1 amplitude	9.0 ± 2.7	5.2 ± 2.5	6.5 ± 2.9	-40 ± 14	< 0.001	2.56
	EPSP 2 amplitude	13.8 ± 3.0	8.7 ± 3.1	10.1 ± 3.7	-38 ± 14	< 0.001	2.66
	PPR	1.58 ± 0.18	1.66 ± 0.29	1.57 ± 0.19	+5 ± 13	0.197	0.42

Mean EPSP amplitudes and paired-pulse ratios (PPR; ± SD) for optically triggered COM afferents challenged with 2 μM 5-HT in control conditions or in the presence of 10 μM SB214461, a blocker of 5-HT_{1B} receptors. P-values are for Student's t-tests for paired samples, while effect sizes are represented by Cohen's *d*.

Table 9. Presynaptic chemogenetic modulation of COM afferents

DREADD	Condition	EPSP 1	EPSP 2	PPR
hM4Di (n = 14)	Baseline	9.4 ± 4.1	14.6 ± 6.8	1.54 ± 0.20
	+CNO (0.05 - 5 μM)	2.5 ± 2.7	4.1 ± 3.6	1.95 ± 0.62
	Percent change	-72 ± 22%	-68 ± 21%	+26 ± 32%
	t-test (p-value)	< 0.001	< 0.001	0.011
	Effect size (Cohen's *d*)	1.99	1.93	0.89
hM3Dq (n = 8)	Baseline	7.8 ± 2.3	12.4 ± 3.9	1.58 ± 0.16
	+ 5 μM CNO	7.4 ± 2.7	11.7 ± 3.6	1.61 ± 0.20
	Percent change	-6 ± 13%	-5 ± 6%	+3 ± 16%
	t-test (p-value)	0.340	0.061	0.704
	Effect size (Cohen's *d*)	0.13	0.18	0.17

Measurements of EPSP amplitudes are from the average of 10 consecutive trials in each experimental condition. P-values are for Student's t-tests for paired samples comparing EPSP amplitudes in baseline conditions and after addition of clozapine-N-oxide (CNO). Effect sizes for ACh effects are represented by Cohen's *d*.

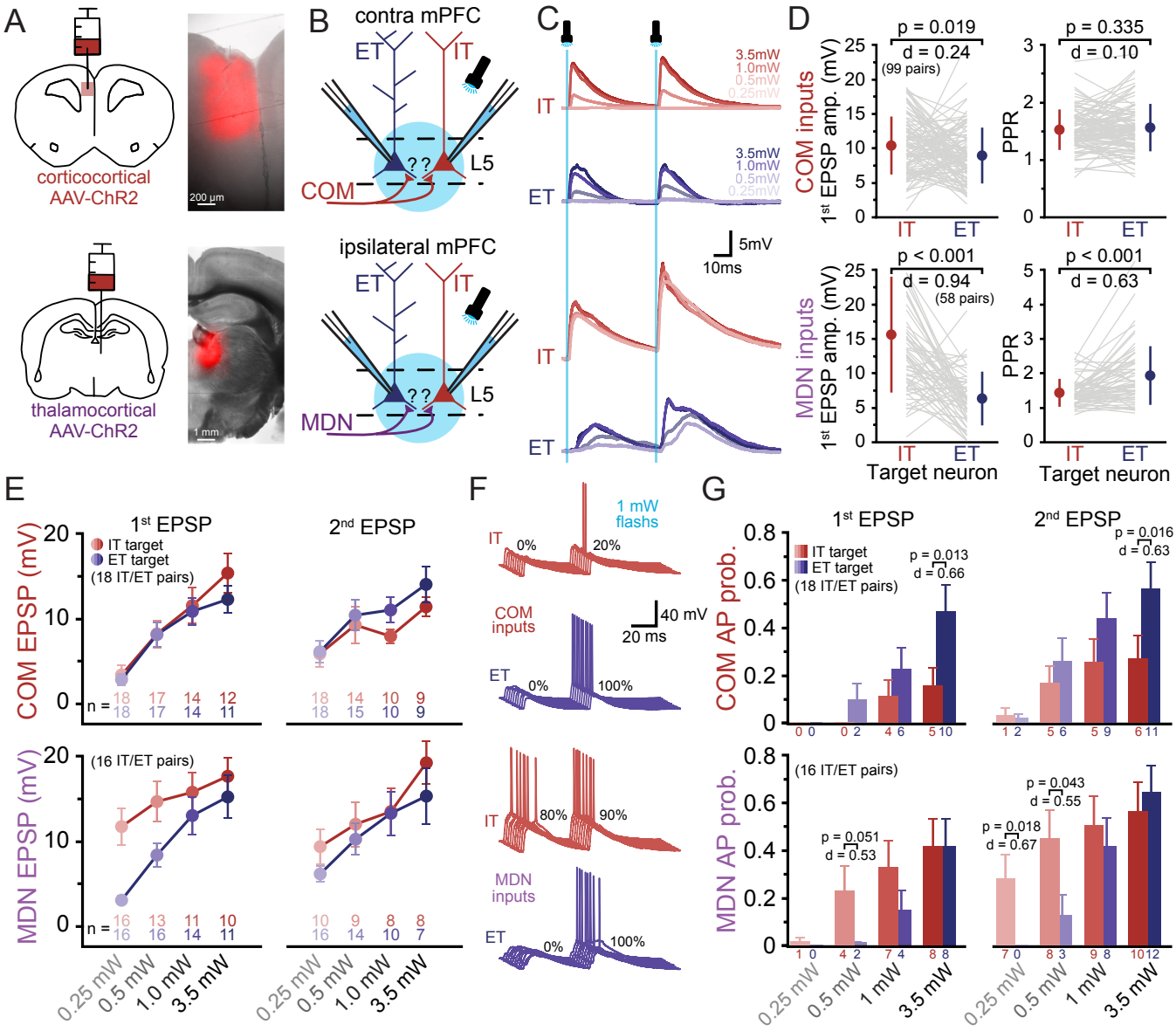

Figure 1. Corticocortical and thalamocortical afferent input to IT and ET neurons in the prelimbic cortex. ***A***, Diagram (left) of approach for delivering ChR2-mCherry to commissural (COM) corticocortical (top) and thalamocortical (MDN; bottom) afferents to the prelimbic cortex, and images of injection sites (right). ***B***, Diagrams of experimental setup for recording light-triggered COM (top) or MDN (bottom) EPSPs in pairs of IT and ET neurons. ***C***, COM (top) and MDN (bottom) EPSPs (averages of 10 consecutive trials) recorded in pairs of IT (red traces) and ET (blue traces) layer 5 neurons in response to two flashes (1 ms) of blue light. ***D***, Comparison of the first EPSP amplitudes (left) and paired-pulse ratios (PPR; right) in pairs of IT (red) and ET (blue) target neurons. ***E***, Comparison of COM (top) and MDN (bottom) mean EPSP amplitudes in response to increasing LED power. The number of data points (neurons) falls off at higher light intensities as some neurons had only suprathreshold EPSPs. ***F***, Ten consecutive trials of COM (top) or MDN (bottom) synaptic activation (1 mW) recorded in pairs of IT (red) and ET (blue) neurons. The proportions (%) of trials exhibiting an AP for each flash are shown. ***G***, Plots of the mean probabilities of action potential (AP) generation (± SEM) across all trials and all IT and ET target neurons in response to increasing LED intensity for COM (top) and MDN (bottom) inputs. Numbers below bars indicate the number of IT (red) and ET (blue) neurons (out of the 18 or 16 neurons per group) that exhibited an AP in at least one trial at the given LED intensity.

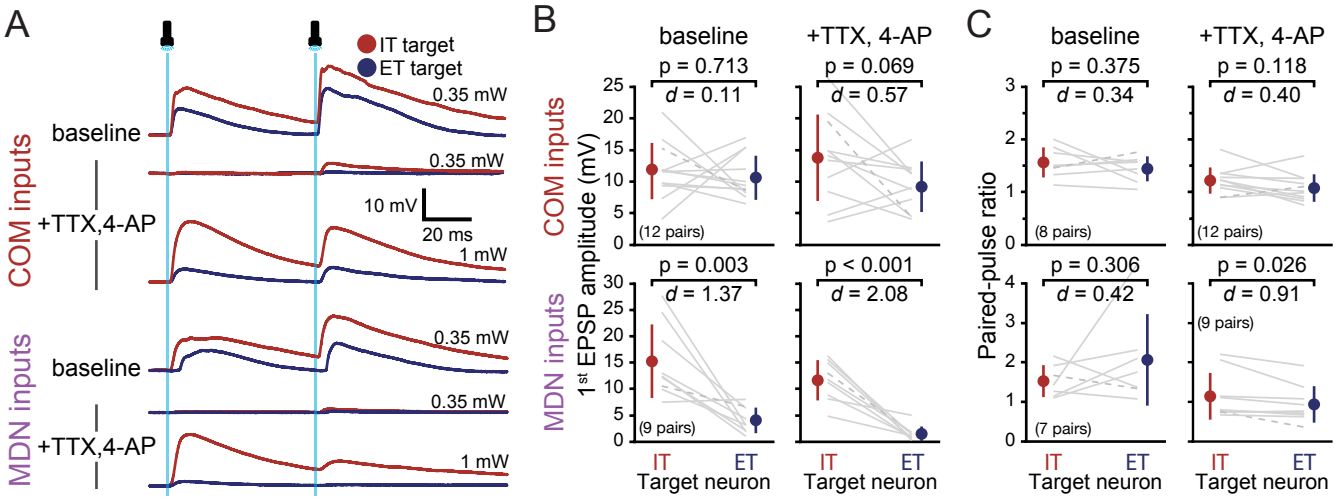

Figure 2. Monosynaptic connectivity of callosal (COM) and thalamocortical (MDN) inputs to IT and ET neurons. ***A***, Average EPSPs (10 consecutive trials) in pairs of IT (red traces) and ET (blue traces) target neurons following activation of COM (upper traces) or MDN (lower traces) afferents in baseline conditions and after application of 1 μM TTX and 100 μM 4-AP at the indicated LED intensities. ***B***, Comparisons of first EPSP amplitudes in IT-ET pairs in baseline conditions and after isolation of monosynaptic inputs with TTX and 4-AP. Gray lines indicate individual neuron pairs, with the dashed lines indicating data for neurons shown in ***A***. Mean values and standard deviations are offset with filled symbols. P-values for Student's t-tests for paired data and effect sizes (Cohen's *d*) are shown. ***C***, Similar to ***B***, but for paired-pulse ratios. In some neurons, the second EPSP was suprathreshold in baseline conditions, leading to a reduction in the number of pairs quantified for PPR in baseline conditions.

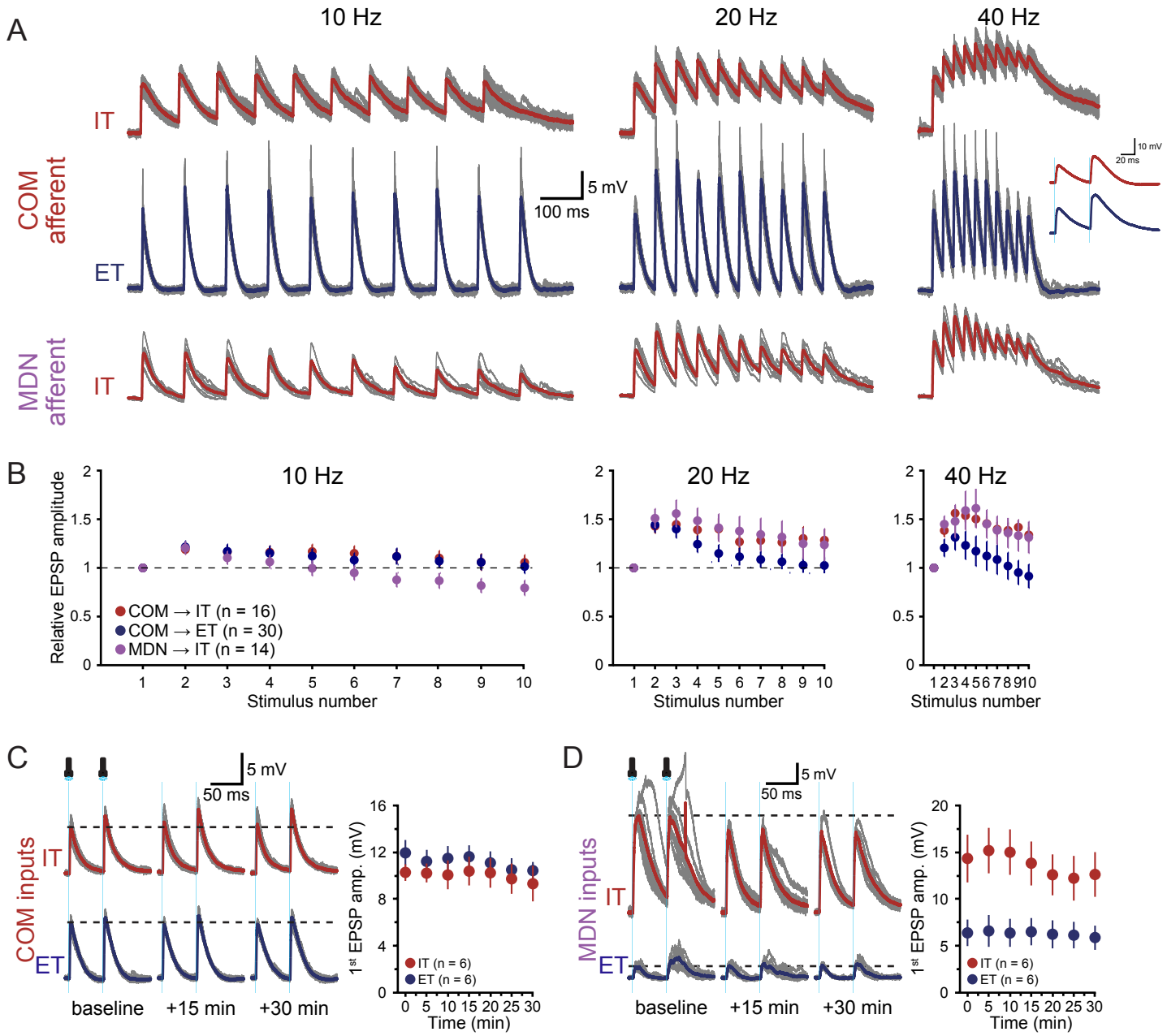

Figure 3. Frequency-dependent short-term plasticity in commissural (COM) and corticothalamic (MDN) inputs to IT and ET neurons and response stability over time. ***A***, Ten consecutive responses (gray traces) and their averages (colored traces) to trains of 10 flashes delivered at 10 (left), 20 (middle), and 40 Hz (right) Hz in a IT-ET pair of target neurons experiencing COM input (top and middle traces) and in a different IT neuron experiencing activation of MDN inputs (lower traces). ***B***, Plots of mean normalized EPSP amplitudes (relative to 1st EPSP; ±SEM) during trains of ten optically evoked EPSPs from COM afferents onto IT and ET neurons (red and blue symbols, respectively; not all data from pairs) and from MDN afferents in IT neurons (purple symbols) at the indicated frequencies. ***C***, Ten consecutive trials (gray traces) and average responses (colored traces) in an IT-ET pair experiencing COM-evoked synaptic input under baseline conditions over a 30 minute period (left) and a summary plot of mean EPSP amplitudes over time (±SEM) for 6 IT and 6 ET neurons (not necessarily in pairs). ***D***, Similar to ***C***, but for optical activation of MDN inputs.

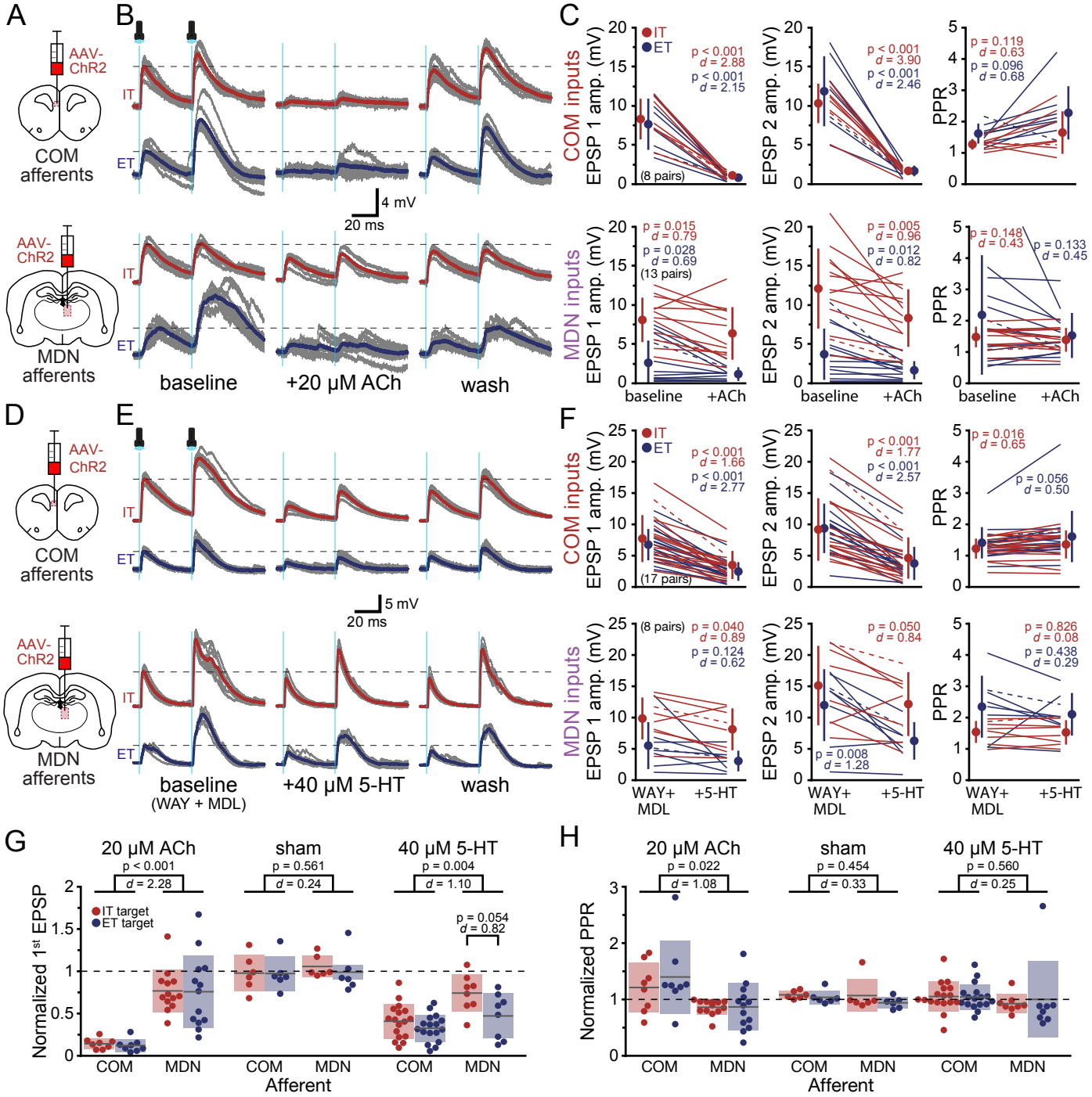

Figure 4. Cholinergic and serotonergic modulation of excitatory afferents in the prelimbic cortex. ***A***, Diagrams of approach for delivering ChR2-mCherry to commissural (COM; top) and thalamocortical (MDN; bottom) afferents to the prelimbic cortex. ***B***, Ten consecutive responses (grey) and their averaged responses (colored thick traces) in pairs of IT (red) and ET (blue) target neurons following activation of COM (top) or MDN (bottom) afferents in baseline conditions (left), after application of 20 μM ACh (middle), and after 15-20 minutes of wash (right). ***C***, Comparisons of EPSP amplitudes (left, middle) and paired-pulse ratios (PPR; right) in IT (red) and ET (blue) target neurons in baseline conditions and in the presence of ACh. Dashed lines indicate data from traces shown in ***B***. Mean values and standard deviations are offset with filled symbols. P-values for Student's t-tests and effect sizes (Cohen's *d*) are color-coded to neuron subtype. ***D-F***, Similar to ***A-C***, but for application of 40 μM 5-HT. For 5-HT experiments, baseline conditions included WAY 100635 (30 nM) and MDL 11939 (500 nM) to block postsynaptic 5-HT receptors. Note that for MDN inputs, responses in ET neurons are largely polysynaptic (see main text). ***G-H***, Comparisons of treatment effects on first EPSP amplitudes and paired-pulse ratios for COM (***G***) and MDN (***H***) inputs to IT and ET neurons. Grey lines indicate means, and shaded areas denote standard deviations. The only large target-dependent effect was for serotonergic effects on MDN afferents (shown).

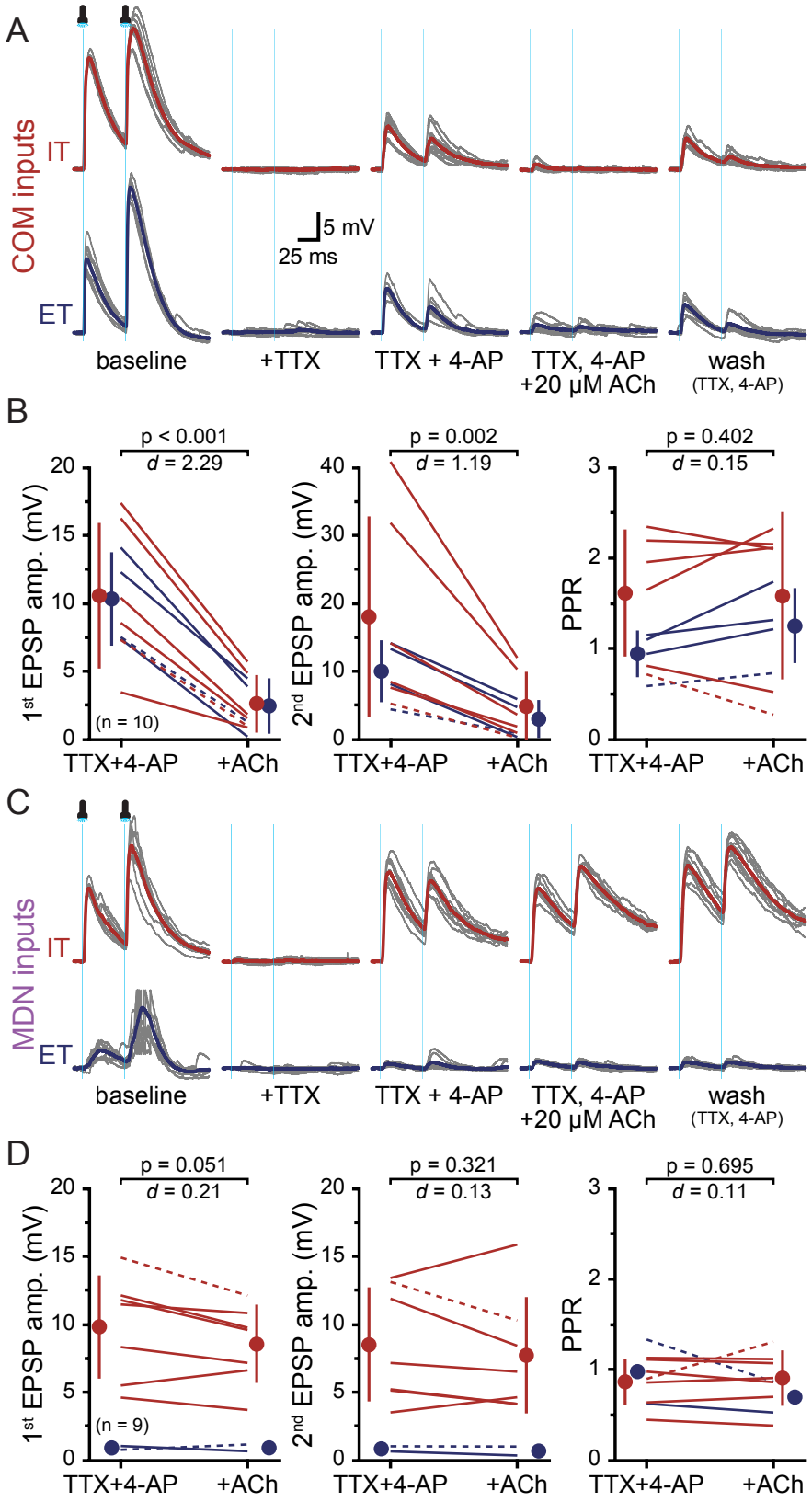

Figure 5. Selective cholinergic suppression of glutamate release from monosynaptic commissural (COM) afferents to IT and ET neurons in prelimbic cortex. ***A***, Ten consecutive optically activated COM EPSP pairs (grey traces) and their averaged responses (colored traces) in a pair of IT (red) and ET (blue) neurons in baseline conditions (left), after sequential and additive applications of 1 μM TTX, 100 μM 4-AP, and 20 μM ACh (with 10 μM eserine; middle traces), and after wash in TTX + 4-AP (right). ***B***, Plots of the effects of 20 μM ACh on COM EPSP amplitudes (left and middle) and paired-pulse ratios (PPR; right). ***C***, Ten consecutive responses (grey) and their averages (colored traces) for optical activation of thalamic (MDN) inputs to a pair of IT (red) and ET (blue) neurons. Note the lack of monosynaptic MDN input to the ET neuron. ***D***, Plots of the effects of 20 μM ACh on MDN EPSP amplitudes (left and middle) and paired-pulse ratios (PPR; right). P-values are for Student's t-tests for paired samples, while effect sizes are represented by Cohen's *d*, and are calculated from all neurons (for IT-only results for MDN inputs, see **Table 7**).

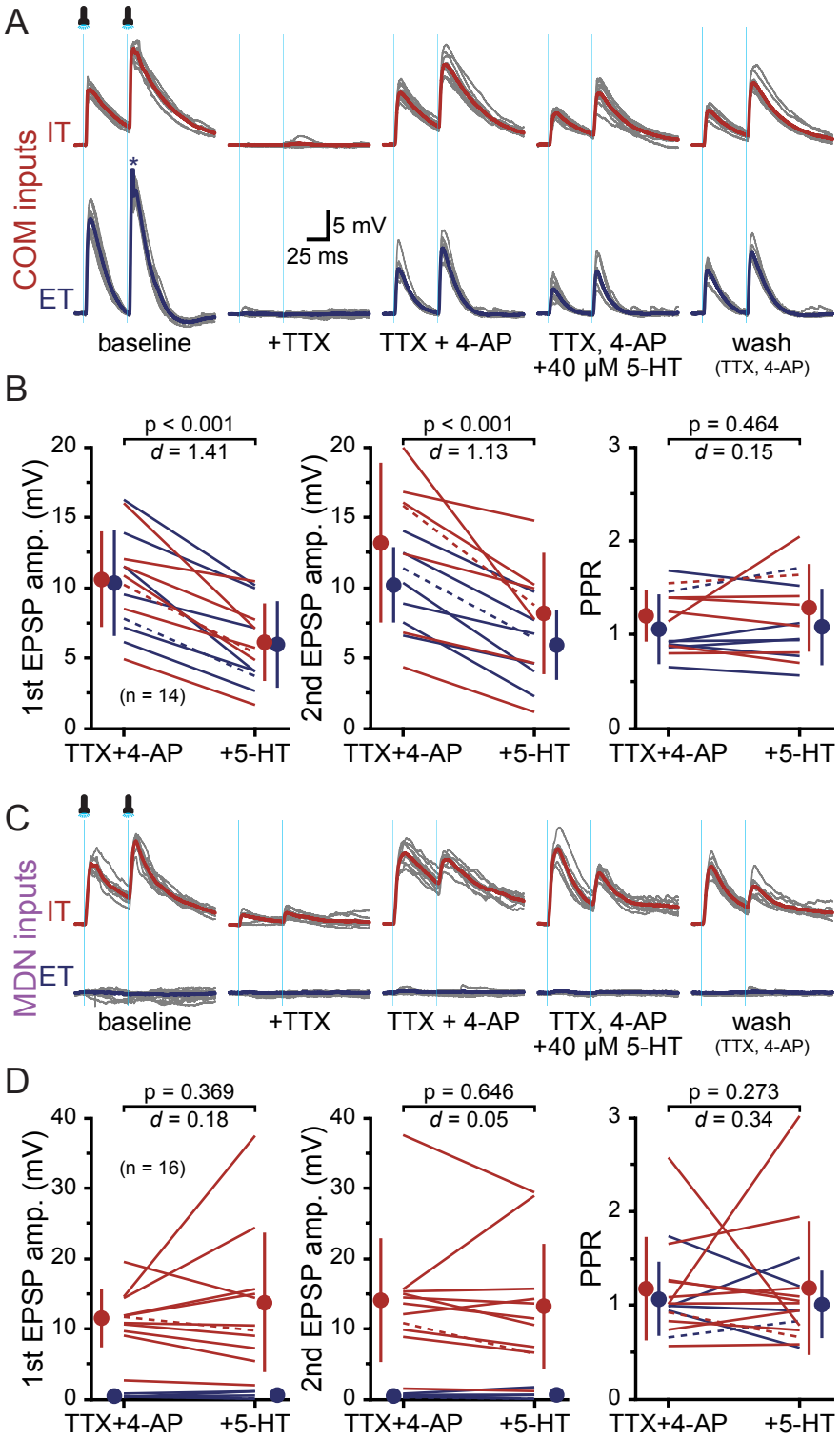

Figure 6. Selective serotonergic suppression of glutamate release from monosynaptic commissural (COM) afferents to IT and ET neurons in prelimbic cortex. ***A***, Ten consecutive optically activated COM EPSP pairs (grey traces) and their averaged responses (colored traces) in a pair of IT (red) and ET (blue) neurons in baseline conditions (left), after sequential and additive applications of 1 μM TTX, 100 μM 4-AP, and 40 μM 5-HT (middle traces), and after wash in TTX + 4-AP (right). ***B***, Plots of the effects of 40 μM 5-HT on COM EPSP amplitudes (left and middle) and paired-pulse ratios (PPR; right). ***C***, Ten consecutive EPSP traces (grey) and their averages (colored traces) for thalamic (MDN) inputs to a pair of IT (red) and ET (blue) neurons. ***D***, Plots of the effects of 40 μM 5-HT on MDN EPSP amplitudes (left and middle) and paired-pulse ratios (PPR; right). P-values are for Student's t-tests for paired samples, while effect sizes are represented by Cohen's *d*, and are calculated from all neurons (for IT-only results for MDN inputs, see **Table 7**).

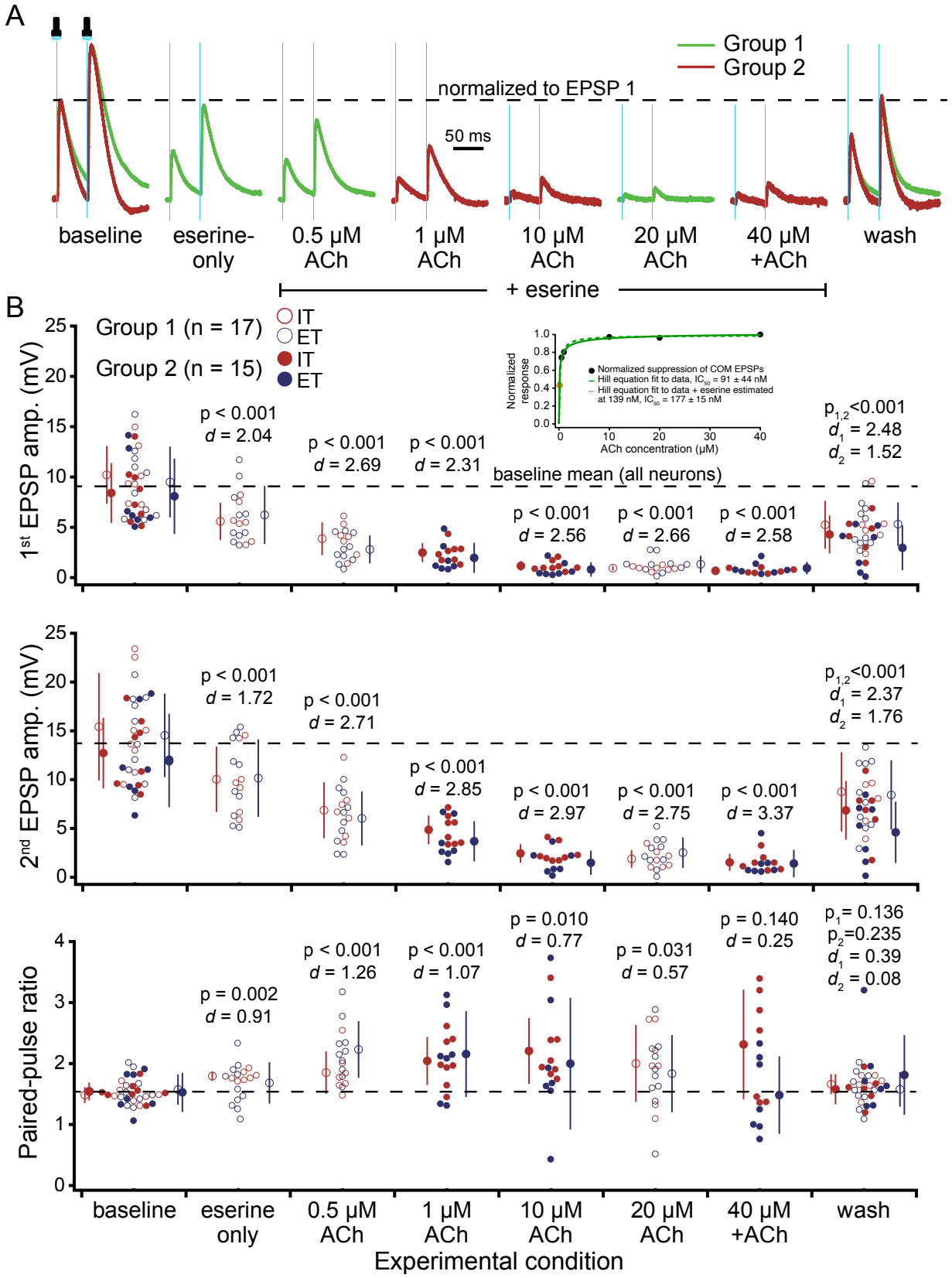

Figure 7. Dose-dependence of cholinergic suppression of excitatory transmission at commissural (COM) afferents. ***A***, Averages of ten consecutive light-evoked COM EPSPs (20 Hz; normalized to baseline EPSP amplitudes) in an IT neuron from "Group 1" and an ET neuron from "Group 2". After recording baseline COM EPSPs, IT and ET neurons in Group 1 received three consecutive treatments consisting of eserine alone (10 μM), eserine with 0.5 μM ACh, and eserine with 20 μM ACh, followed by 10 or more minutes of wash. Group 2 IT and ET neurons were exposed to eserine combined with three increasing doses of ACh (1, 10, and 40 μM). Each dose was applied for 7 minutes. Inset is a plot of normalized responses vs ACh concentrations fit with a Hill equation for raw data (solid green line) and after estimating the eserine-only concentration at 139 nM (orange data point and dashed green line). ***B***, Plots of EPSP amplitudes (top two graphs) and paired-pulse ratios (bottom graph) for each neuron in the various drug conditions (as measured from averages of final 10 responses per condition) for IT (red) and ET (blue) neurons in group 1 (open symbols) and Group 2 (closed symbols). Mean response amplitudes and standard deviations for each condition indicated by larger symbols to the left (IT; red) and right (ET; blue) of each condition. P-values and Cohen's *d* for each drug condition are relative to baseline measurements for the given group. Neurons not necessarily recorded in pairs.

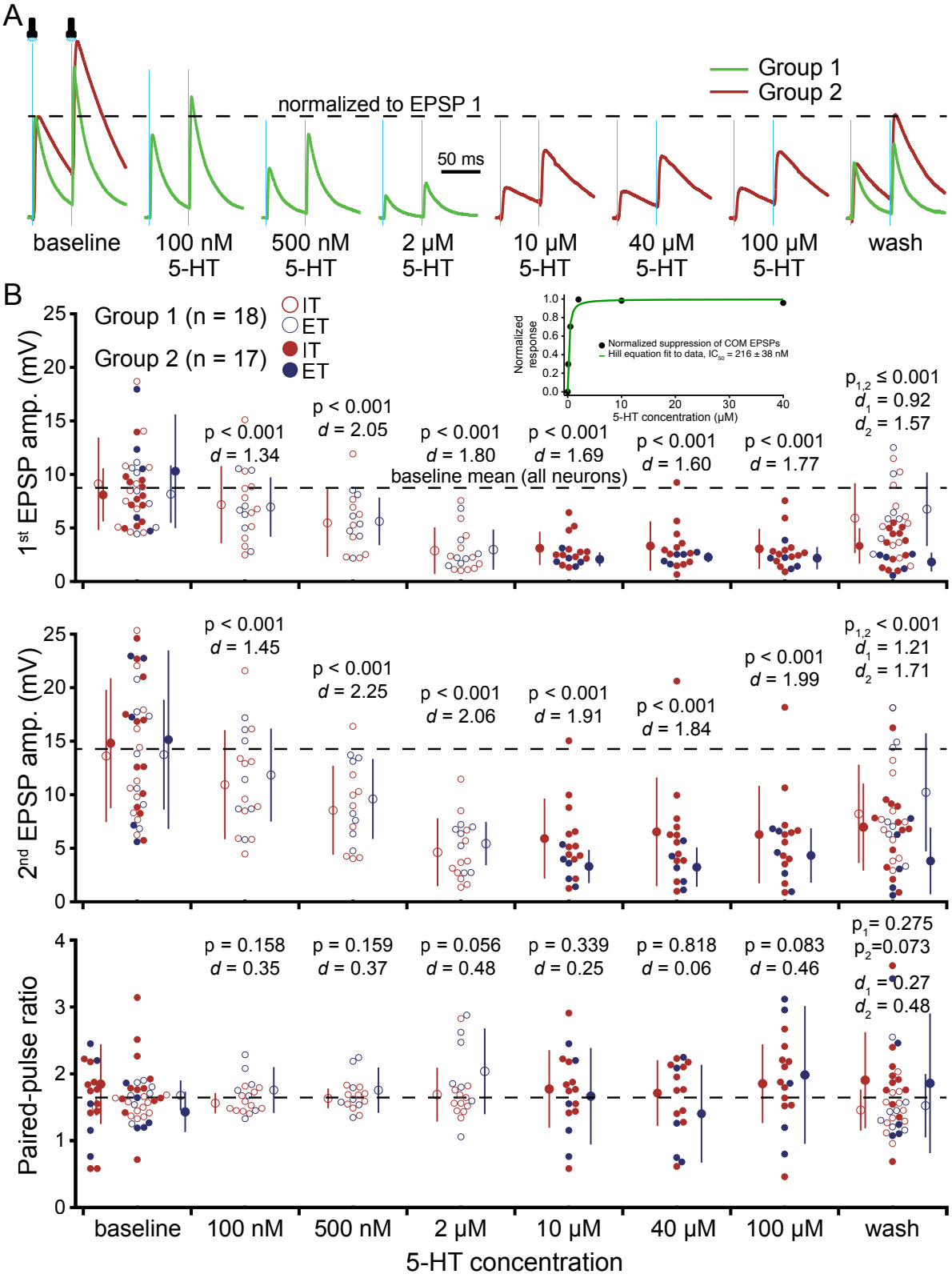

Figure 8. Dose-dependence of serotonergic suppression of excitatory transmission at commissural (COM) afferents. ***A***, Averages of ten consecutive light-evoked COM EPSPs (20 Hz; normalized to baseline EPSP amplitudes) in two IT neurons (one from "Group 1" and one from "Group 2"). After recording baseline COM EPSPs, IT and ET neurons in Group 1 received three consecutively increasing doses of 5-HT (100 nM, 500 nM, and 2 μM) followed by 10 or more minutes of wash in the absence of drugs. Group 2 IT and ET neurons were consecutively exposed to 10, 40, and 100 μM 5-HT, before a similar wash. Inset is a plot of normalized responses vs 5-HT concentration fit with a Hill equation. ***B***, Plots of EPSP amplitudes (top two graphs) and paired-pulse ratios (bottom graph) for each neuron in the various drug conditions (as measured from the averages of ten consecutive trials per condition) for IT (red) and ET (blue) neurons in group 1 (open symbols) and Group 2 (closed symbols). Mean response amplitudes and standard deviations for each condition indicated by larger symbols to the left (IT; red) and right (ET; blue). Data from one Group 2 neuron with PPR values above 4 (4.8, 9.5, 4.6, and 6.4, respectively, for 10 μM, 40 μM, 100 μM, and wash) were excluded for calculations of mean and standard deviation and are not shown in plot. An additional pair of group 2 neurons was not exposed to 40 μM 5-HT. P-values and Cohen's *d* for each drug condition are relative to baseline measurements for the given group. Neurons were not necessarily recorded in pairs.

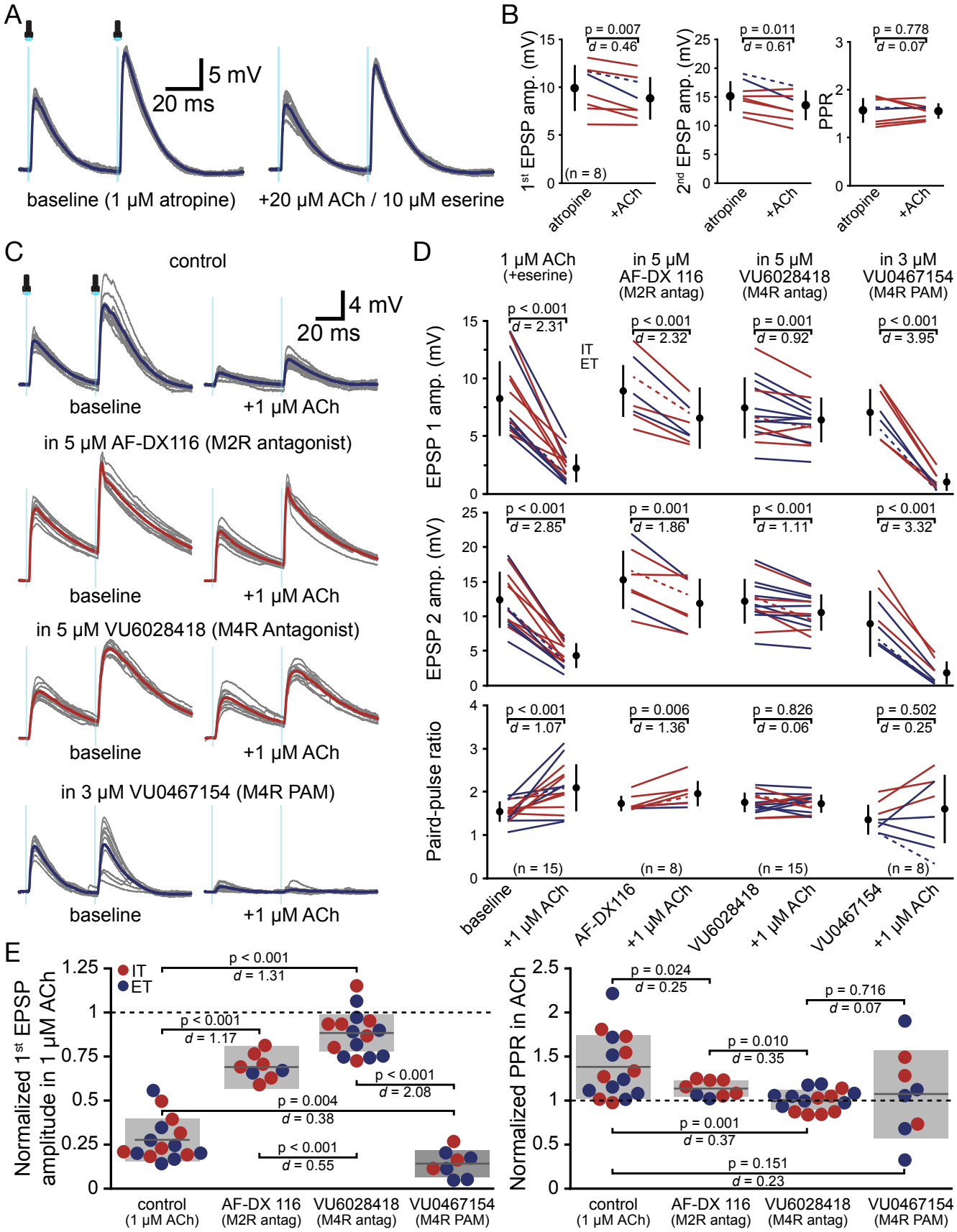

Figure 9. M4 muscarinic receptors mediate cholinergic suppression of commissural (COM) synaptic transmission. ***A***, Ten consecutive responses to optical activation of COM afferents (two 1-ms flashes at 20 Hz; grey traces) and averaged responses (blue traces) in an ET neuron in the presence of 20 μM atropine (a non-specific muscarinic receptor blocker; left) and after addition of 20 μM ACh (with 10 μM eserine; right). ***B***, Summary plots of EPSP amplitudes (left and middle) and paired-pulse ratios (PPR; right) in baseline conditions with atropine present and after addition of ACh for eight neurons. Individual neurons shown with lines, with means and standard deviations for the different conditions offset. Dashed lines indicate data from neuron shown in ***A***. ***C***, Ten consecutive COM responses (grey) and averaged responses (colored traces) in IT (red) or ET (blue) neurons in various baseline conditions (as indicated; left) and after addition of 1 μM ACh (with 10 μM eserine; right). The top trace shows control experiments conducted in regular aCSF, while the other neurons were pre-exposed to M2- or M4-specific antagonists (middle traces) or an M4-specific positive allosteric modulator (PAM; lower traces), as indicated. ***D***, Plots of the effects of 1 μM ACh with eserine on COM EPSP amplitudes (top and middle) and paired-pulse ratios (PPR; bottom) for the different experimental conditions. Dashed lines indicate results from the neurons shown in ***C***. ***E***, Plots of the normalized first EPSP amplitudes (relative to baseline EPSPs; left) and PPR (right) in the presence of ACh for the different experimental conditions. Grey lines show means, grey shaded areas indicate standard deviations. P-values (Student's t tests) and effect sizes (Cohen's *d*) are indicated.

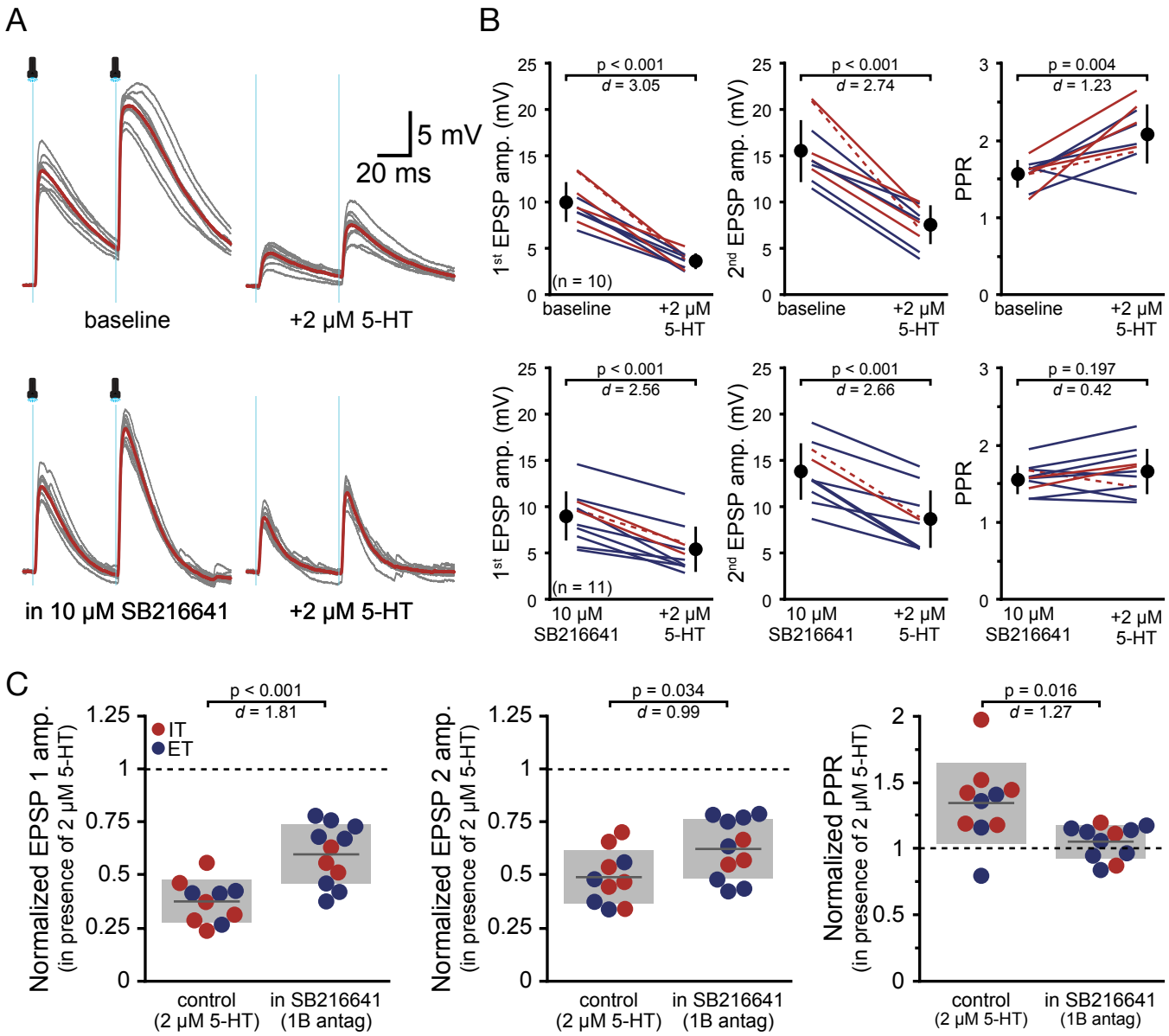

Figure 10. Contribution of 5-HT$_{1B}$ (1B) receptors to serotonergic modulation of commissural (COM) synaptic transmission. ***A***, Ten consecutive responses to optical activation of COM afferents (two 1-ms flashes at 20 Hz; grey traces) and averaged responses (red traces) in two IT neurons in baseline conditions (left) and after addition of 2 μM serotonin (5-HT; right) in control conditions (top neuron) and in the continued presence of 10 μM SB216641 (a 1B antagonist; bottom neuron). ***B***, Summary plots of EPSP amplitudes (left and middle) and paired-pulse ratios (PPR; right) in baseline conditions and in the presence of 5-HT. Individual neurons shown with lines, with means and standard deviations for the different conditions offset. Dashed lines indicate data from neurons shown in ***A***. ***C***, Plots of the normalized first EPSP amplitudes (relative to baseline EPSPs; left and middle) and PPR (right) in the presence of 5-HT for control neurons and those exposed to SB214461. Grey lines show means, grey shaded areas indicate standard deviations. P-values (Student's t tests) and effect sizes (Cohen's *d*) are indicated.

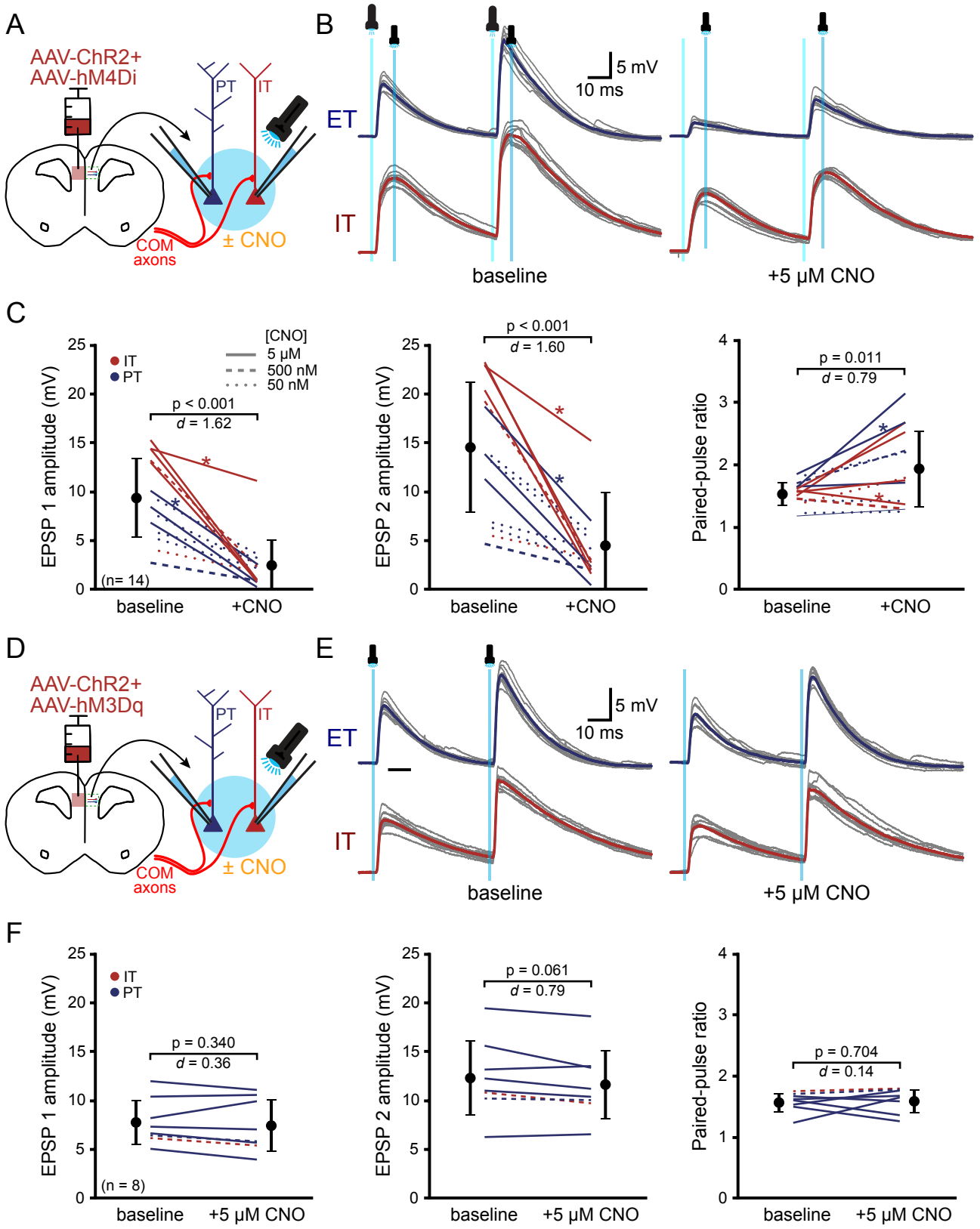

Figure 11. Activation of selectively expressed $G_{i/o}$, but not G_q, presynaptic metabotropic receptors suppresses commissural (COM) synaptic transmission. ***A***, Diagram of experimental setup, with AAV-induced co-expression of channelrhodopsin-2 (ChR2) and hM4Di ($G_{i/o}$-coupled) receptors in one cerebral hemisphere and subsequent optical activation of COM afferents in the opposite hemisphere before and after the application of clozapine-N-oxide (CNO). ***B***, Ten consecutive responses to pairs (20 Hz) of COM afferent activations (grey traces) and their averaged responses (colored traces) in a pair of IT (red) and ET (blue) neurons in baseline conditions (left) and after addition of 5 μM CNO (right). ***C***, Comparisons of EPSP amplitudes (left and middle) and paired-pulse ratios (PPR; right) before and after CNO applications at the noted concentrations for 14 neurons. Mean responses (± SD) shown with offset symbols. P-values (Student's t-tests for paired data) and effect sizes (Cohen's *d*) shown for each. Asterisks indicate data from panel ***B***. ***D-F***, Similar to ***A-C***, but for co-expression of ChR2 and hM3Dq, a G_q-coupled receptor for CNO. In panel ***F***, dashed lines indicate data from experiments shown in panel ***E***.

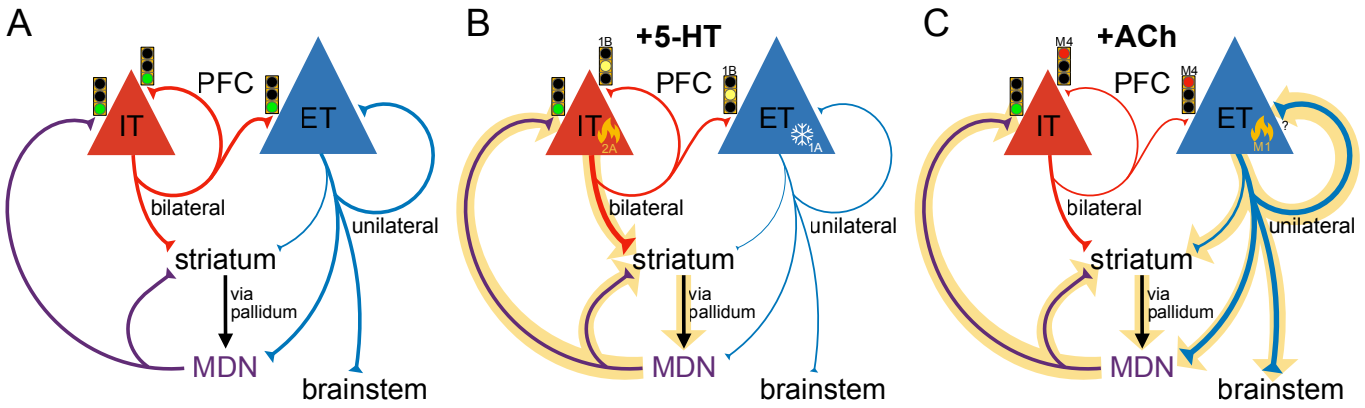

Figure 12. Circuit-level impact of 5-HT and ACh release in the prefrontal cortex. ***A***, Diagram of local and long-distance circuits subserved by IT (red) and ET (blue) neurons in the prefrontal cortex (PFC). IT neurons project bilaterally within the cortex and to the striatum (specifically the dorsomedial striatum and nucleus accumbens), while networks of interconnected ET neurons project ipsilaterally within the cortex, moderately to the striatum, and to one or more subcortical targets (e.g., the brainstem and/or the mediodorsal nucleus [MDN] of the thalamus). The MDN is bidirectionally connected with the striatum (projecting direct efferents and receiving feedback via the pallidum) and with the cortex (selectively targeting IT neurons in the PFC and receiving feedback via ET projections and striatal circuits). Green traffic lights indicate normal synaptic transmission in the absence of neuromodulation. ***B***, 5-HT increases the gain of IT neurons via 2A receptors and strongly inhibits ET neurons via 1A receptors, while moderately suppressing IT-derived corticocortical communication (yellow traffic symbols), perhaps via presynaptic 1B receptors. The net effect is preferential amplification of thalamocortically driven corticostriatal output bilaterally, which in turn may provide feedback to the MDN via the pallidum. ***C***, In the presence of ACh, M4 receptors strongly suppress IT-derived corticocortical communication (red traffic lights) while M1 receptors preferentially enhance the gain of interconnected ET neurons, promoting corticofugal output to the ipsilateral striatum and deep structures, including the MDN, which in turn promotes bilateral corticostriatal output via IT neurons.